EuroIntervention 2023;19:222-231 published online ahead of print April 2023

First-in-human evaluation of a novel ultrathin sirolimus-eluting iron bioresorbable scaffold: 3-year outcomes of the IBS-FIM trial

Runlin Gao[1]*, MD; Bo Xu[1,2], MBBS; Zhongwei Sun[1], MSc; Changdong Guan[1], MSc; Lei Song[1], MD; Lijian Gao[1], MD; Chongjian Li[1], MD; Jingang Cui[1], MD; Yin Zhang[1], MD; Kefei Dou[1], MD; Jue Chen[1], MD; Chaowei Mu[1], MD; Haibo Liu[1], MD; Ang Li[1], BS; Zihao Li[1], MSc; Lihua Xie[1], MSc; Yuejin Yang[1], MD; Shubin Qiao[1], MD; Yongjian Wu[1], MD; Gregg W. Stone[3], MD

1. Department of Cardiology, National Clinical Research Center for Cardiovascular Diseases, National Center for Cardiovascular Diseases & Fuwai Hospital, Chinese Academy of Medical Sciences & Peking Union Medical College, Beijing, People's Republic of China; 2. National Clinical Research Center for Cardiovascular Diseases, Fuwai Hospital Chinese Academy of Medical Sciences, Shenzhen, People's Republic of China; 3. The Zena and Michael A. Wiener Cardiovascular Institute, Icahn School of Medicine at Mount Sinai, New York, NY, USA

R. Gao, B. Xu, and Z. Sun contributed equally to this work.

This paper also includes supplementary data published online at: https://eurointervention.pcronline.com/doi/10.4244/EIJ-D-22-00919

KEYWORDS

- bioresorbable scaffolds
- intravascular ultrasound
- optical coherence tomography
- prior percutaneous intervention
- QCA

Abstract

Background: The first-generation polymeric bioresorbable scaffolds resulted in higher than acceptable 3-year rates of device-related adverse outcomes.

Aims: We aimed to assess the intermediate-term safety and performance of a novel ultrathin-strut sirolimus-eluting iron bioresorbable scaffold (IBS) in non-complex coronary lesions.

Methods: The prospective, single-arm, open-label IBS first-in-human study enrolled 45 patients, each with a single *de novo* lesion. Enrolled patients were randomly assigned to 2 follow-up cohorts. Angiographic and imaging follow-up with intravascular ultrasound and optical coherence tomography (OCT) were conducted at 6 and 24 months in cohort 1 (n=30) and at 12 and 36 months in cohort 2 (n=15). Clinical follow-up was conducted at 1, 6 and 12 months, and annually thereafter up to 5 years. The coprimary outcomes were target lesion failure (TLF) and angiographic late lumen loss (LLL) at 6 months.

Results: A total of 45 patients were enrolled between April 2018 and January 2019. The mean age was 53.2 years, 77.8% were male, and 26.7% had diabetes. The TLF rates were 2.2% at 6 months and 6.7% at 3 years, which in all cases were due to clinically indicated target lesion revascularisation. No deaths, myocardial infarctions or stent thromboses occurred during 3-year follow-up. In-scaffold LLL was 0.33±0.27 mm at 6 months and 0.37±0.57 mm at 3 years. By OCT, the proportion of covered struts was 99.8% at 6 months and 100% after 1 year. The 3-year strut absorption rate was 95.4%.

Conclusions: In this first-in-human experience, an ultrathin IBS was safe and effective for the treatment of *de novo* non-complex coronary lesions up to 3-year follow-up.

**Corresponding author: Department of Cardiology, National Clinical Research Center for Cardiovascular Diseases, National Center for Cardiovascular Diseases & Fuwai Hospital, Chinese Academy of Medical Sciences & Peking Union Medical College, 167 Beilishi Road, 100037 Beijing, People's Republic of China. E-mail: gaorunlin@citmd.com*

SUBMITTED ON 19/10/2022 - REVISION RECEIVED ON 1st 30/12/2022 / 2nd 02/02/2023 - ACCEPTED ON 28/02/2023

DOI: 10.4244/EIJ-D-22-00919

Abbreviations

BRS	bioresorbable scaffolds
DES	drug-eluting stents
IVUS	intravascular ultrasound
LLL	late lumen loss
MLD	minimum lumen diameter
OCT	optical coherence tomography
PoCE	patient-oriented clinical endpoint
QCA	quantitative coronary angiography
RVD	reference vessel diameter
TLF	target lesion failure

Introduction

Bioresorbable scaffolds (BRS) were introduced to address the long-term limitations of permanent metallic drug-eluting stents (DES), which include vascular inflammation, reactive dysmotility, neoatherosclerosis, and side branch jailing[1,2]. After providing temporary scaffolding and eluting an antiproliferative agent to inhibit excessive neointimal hyperplasia, the BRS is completely resorbed, "uncaging" the treated vessel to restore its capabilities for vascular adaptation and vasomotion[3]. However, large clinical trials of a first-generation thick-strut (~157 µm) polymer-based everolimus-eluting BRS (Absorb bioresorbable vascular scaffold [BVS]; Abbott) demonstrated increased rates of device thrombosis and myocardial infarction (MI) during the 3-year resorption window[4-6]. Suboptimal scaffold expansion − due to its thick struts, recoil and limited expansion capability – was largely responsible for the increase in early scaffold thrombosis, while in many cases, scaffold discontinuities and intraluminal scaffold dismantling, caused by uneven degradation during the bulk erosion process, contributed to late and very late scaffold thromboses[2,7]. Thus, a search ensued for alternate materials capable of reducing scaffold thickness while optimising the degradation process[8]. A bioabsorbable magnesium-based scaffold (AMS-1; first- and second-generation DREAMS; BIOTRONIK AG) was introduced and iterated, although safety and effectiveness concerns were raised given its thick struts (150 µm), premature absorption, loss of radial force, and post-resorption amorphous calcium phosphate residues[3,9-11].

Iron was suggested as an alternative bioresorptive metal in scaffolds. Iron is biocorrodible, has a strong radial force, acceptable malleability and plays a vital physiological role in human physiology. In animal studies, pure iron and nitride iron scaffolds have been shown to be safe and biocompatible[12-16]. A novel sirolimus-eluting iron bioresorbable scaffold (IBS; Biotyx Medical, previously developed at Lifetech Scientific Company) has been developed, consisting of an ultrathin (70 µm) nitriding iron backbone with a zinc submicron layer, coated with poly-D,L-lactic acid (PDLLA) incorporating sirolimus[17,18]. In porcine studies biocorrosion did not occur before 6 months, and strut coverage was more rapid than with the cobalt-chromium everolimus-eluting stent (EES; XIENCE PRIME; Abbott), while other vascular responses were similar[19]. We, therefore, performed a first-in-human trial (IBS-FIM; ClinicalTrials.gov: NCT03509142) using multimodality imaging, including quantitative coronary angiography (QCA), intravascular ultrasound (IVUS) and optical coherence tomography (OCT), to assess the feasibility, bioresorption, and potential safety and effectiveness of IBS for the treatment of patients with coronary artery disease.

Editorial, see page 193

Methods

STUDY DESIGN

IBS-FIM was a prospective, single-arm, open-label trial that enrolled 45 patients from Fuwai Hospital in Beijing, People's Republic of China. To acquire serial intravascular imaging information at different intervals, the population was randomly divided in a 2:1 ratio into 2 cohorts. The 30 patients randomised to cohort 1 were assigned to undergo imaging follow-up at 6 months and 2 years, and the 15 patients randomised to cohort 2 were assigned to undergo follow-up imaging at 1 year and 3 years. Assessment using IVUS and OCT was performed post-procedure and at each of the angiographic follow-up time points. The protocol was reviewed and approved by the ethics committee at Fuwai Hospital.

PARTICIPANTS

Eligible subjects were between 18 and 75 years of age and had evidence of myocardial ischaemia indicating percutaneous coronary intervention (PCI). Angiographic inclusion criteria required the presence of a single target lesion that could be covered with a single study scaffold, with a target lesion length ≤18 mm, diameter stenosis (DS) ≥70% in a vessel with reference vessel diameter (RVD) between 3.0 and 3.5 mm by visual estimation and with Thrombolysis In Myocardial Infarction (TIMI) flow grade ≥1. Patients were excluded if they presented with acute myocardial infarction (MI), had undergone stent implantation in the target vessel within 1 year, had prior coronary artery bypass graft surgery (CABG) or had contraindications for CABG, had severe heart failure, or had a left ventricular ejection fraction (LVEF) <40%. The complete list of inclusion and exclusion criteria appears in **Supplementary Appendix 1**. All subjects provided written informed consent.

STUDY DEVICE

The ultrathin-strut (70 µm) sirolimus-eluting IBS consists of an ultrathin (53 µm) nitriding iron (Fe-0.05%N) backbone, with a pure zinc submicron layer as a sacrifice anode to delay the onset of backbone degradation, and a PDLLA coating with sirolimus to deliver the drug and create a local low pH environment that accelerates the corrosion of the iron struts into soluble iron ions by polymer degradation once the zinc is exhausted[17,18]. Two sets of gold radiopaque markers are located at both ends of the scaffold **(Supplementary Figure 1)**. The drug loading density is 8 µg per mm of scaffold length, and the drug is completely eluted by 24 weeks. An asymmetric polymer matrix favours elution of the drug to the abluminal compartment.

The IBS is currently manufactured with diameters of 3.0 and 3.5 mm and lengths of 15, 18, and 23 mm. The integrity and

scaffold force are maintained during the first 3 months[18], after which it locally degrades into iron ions which diffuse into tissue and precipitate as particulates in the vessel wall **(Supplementary Figure 2)**. The particulates are then transferred into haemosiderin by macrophages and are cleared by the lymphatic system for recycling[15,17,19]. The iron content in a 3.0 mm diameter x 18 mm long IBS is 9 mg, which corresponds to the amount in approximately 20 ml of blood, or the weekly iron intake of an adult.

PROCEDURE

Subjects received dual antiplatelet therapy (DAPT; clopidogrel 75 mg/day and aspirin 100 mg/day), beginning at least 3 days pre-procedure. Predilation of the target lesion with balloon angioplasty was required. After stenting, DAPT with clopidogrel (75 mg/day) or ticagrelor (90 mg twice daily) was prescribed for at least 12 months and aspirin (100 mg/day) was administered lifelong.

FOLLOW-UP

Clinical follow-up was conducted for all study participants at 1, 6 and 12 months, and yearly thereafter until 5 years. Subjects in cohort 1 underwent angiography, IVUS and OCT at 6-month and 2-year follow-up, while subjects in cohort 2 underwent the same assessments at 1-year and 3-year follow-up. In addition to standard assessments, OCT was used to semiquantitatively assess the *in vivo* degradation of the IBS as described below. At the present time clinical and imaging follow-up are completed up to 3 years.

ENDPOINTS

The primary endpoints were target lesion failure (TLF: a composite of cardiac death, target vessel-related myocardial infarction [TV-MI] or clinically indicated target lesion revascularisation [CI-TLR]) and late lumen loss (LLL) by QCA at 6 months. Secondary endpoints included the rates of device, lesion, and clinical success immediately post-procedure; the patient-oriented clinical endpoint (PoCE), a composite of all-cause death, all MI, or any revascularisation; the components of TLF; and scaffold thrombosis. Other QCA endpoints included in-scaffold and in-segment acute recoil, RVD, minimum lumen diameter, percentage DS, binary restenosis, and vasomotion as assessed by QCA. IVUS endpoints included the vessel area, lumen area, scaffold area, neointimal area, percentage area obstruction, volumetric obstruction and late recoil area. OCT endpoints included strut coverage, area obstruction, late recoil and scaffold absorption. Detailed definitions of the endpoints are provided in **Supplementary Appendix 2**. All clinical endpoint events were adjudicated by a clinical events committee, independent from the investigators and sponsor.

IMAGING ASSESSMENTS

QCA, IVUS and OCT analyses were performed at the core laboratory at Fuwai Hospital. QCA analysis was performed using CAAS Workstation 8.1 (Pie Medical Imaging) as previously described[20]. IVUS (OptiCross; Boston Scientific) was performed at an automated pullback speed of 0.5 mm/s and was analysed in 0.5 mm intervals by QIvus 3.0 (Medis Medical Imaging). Strut absorption on IVUS images was analysed at 1 mm intervals and categorised as obvious versus non-obvious according to the presence of a widening strut shadowing of >300 μm **(Supplementary Figure 3)**. OCT image acquisitions were performed using the C7-XRTM frequency-domain system and Dragonfly imaging catheter (both Abbott). OCT images were acquired at 100 frames/s at a pull-back speed of 20 mm/s. Cross-sectional OCT images were analysed at 0.4 mm intervals by QIvus 3.0 as previously described[20,21]. The absorption process of the IBS was semiquantitatively analysed by OCT, using a novel method[22]. Using postprocedural radial heights of the sharply delineated struts as reference, the struts at follow-up were categorised into 5 groups according to the height of the expanded bow area generated during the degradation process **(Supplementary Figure 4)**. All images were analysed offline by an independent core laboratory (Interventional Cardiovascular Imaging Core Laboratory, National Center for Cardiovascular Diseases, Beijing, People's Republic of China) as previously described[22]. The full quantitative measurement and analysis methods are included in **Supplementary Appendix 2**.

STATISTICAL ANALYSIS

The objective of this pilot study was to evaluate the feasibility and the preliminary safety and effectiveness outcomes of the IBS and to generate data to aid the design of subsequent large-scale, multicenter, randomised controlled clinical trials. The sample size of 45 patients was defined according to the requirements of the Center for Medical Device Evaluation, National Medical Products Administration in China, and was not powered for any specific endpoint. Categorical variables are presented as proportions and were compared using the Chi-square and Fisher's exact tests. Continuous data are presented as mean±standard deviation and were compared using paired t-tests. Missing data were not replaced. Significance was set at a 2-sided α=0.05. All analyses were performed with SAS software v9.4 (SAS Institute).

Results

PATIENTS AND PROCEDURES

Between April 2018 and January 2019, 45 patients (mean age 53.2 years, 77.8% male) with a single qualifying coronary artery lesion were enrolled and randomly assigned to imaging cohort 1 (n=30) or cohort 2 (n=15) after IBS implantation **(Supplementary Figure 5)**. Because of scheduling issues, two patients in cohort 1 crossed over to the imaging follow-up timing of cohort 2. Thus, the imaging results are reported as 28 patients for cohort 1 and 17 patients for cohort 2.

Baseline characteristics are shown in **Supplementary Table 1**. By QCA the mean RVD and lesion length were 2.98±0.38 mm and 14.0±4.2 mm, respectively; 64.4% of lesions were in the left anterior descending (LAD) coronary artery. All lesions underwent predilatation, and 93.3% underwent post-dilatation. Device success occurred in 45 patients (100%). In one patient, a bailout IBS scaffold was required because of an edge dissection after the first

IBS implant; the second scaffold was placed distally to overlap the first scaffold by several mm. There were no procedural complications, and lesion and procedural success were achieved in 100% of patients. Medications at discharge and during follow-up appear in **Supplementary Table 2**.

CLINICAL OUTCOMES

All patients completed follow-up up to 3 years. Clinical outcomes are reported in **Table 1**. Four patients underwent TLR, three of which were clinically indicated. One patient experienced chest discomfort and palpitations at 6 months post-procedure. Angiography showed in-scaffold restenosis in the mid-LAD, and the patient underwent CI-TLR with a metallic DES. Two patients with recurrent angina had restenosis noted at the 12-month angiographic follow-up and underwent CI-TLR. Thus, the rates of TLF (and CI-TLR) were 2.2% at 6 months and 6.7% after 1 year. One additional patient underwent a non-TLR target vessel revascularisation (TVR). The detailed description of the cases of TLR and this TVR are included in **Supplementary Appendix 3**. There were no deaths, MIs or scaffold thromboses up to 3-year follow-up.

Table 1. Clinical outcomes at 3 years.

	6 months n=45	1 year n=45	2 years n=45	3 years n=45
Target lesion failure	1 (2.2)	3 (6.7)	3 (6.7)	3 (6.7)
Patient-oriented composite endpoint	2 (4.4)	4 (8.9)	4 (8.9)	5 (11.1)
All-cause death	0	0	0	0
Cardiac death	0	0	0	0
Myocardial infarction	0	0	0	0
Target vessel myocardial infarction	0	0	0	0
Any revascularisation	2 (4.4)	4 (8.9)	4 (8.9)	5 (11.1)
Clinically indicated TVR	2 (4.4)	4 (8.9)	4 (8.9)	4 (8.9)
Clinically indicated TLR	1 (2.2)	3 (6.7)	3 (6.7)	3 (6.7)
Definite or probable device thrombosis	0	0	0	0

Data are number (%). TLR: target lesion revascularisation; TVR: target vessel revascularisation

QCA RESULTS

Baseline and post-procedure QCA results were similar between the 2 cohorts **(Table 2, Supplementary Table 1).** Acute recoil was 0.12±0.08 mm. Angiographic follow-up was completed in 100% of patients at 6 months and 12 months, in 75.0% of patients at 2 years, and in 47.1% of patients at 3 years **(Supplementary Figure 5)**. As shown in **Table 2** and **Figure 1**, in-scaffold LLL was 0.33±0.27 mm at 6 months, 0.39±0.50 mm at 12 months, 0.40±0.31 mm, at 24 months, and 0.37±0.57 mm at 36 months. In paired analyses there was no significant increase in in-scaffold LLL from 6 months to 24 months (cohort 1: 0.31±0.26 mm and 0.40±0.31 mm respectively; p=0.06) nor from 12 months to 36 months (cohort 2: 0.14±0.15 mm and 0.37±0.57 mm, respectively; p=0.26). Other paired QCA data in cohorts 1 and 2 are shown in **Supplementary Table 3**. Binary restenosis occurred in 3 patients (6.7%) up to 3 years. Vasomotion did not change from 6 months to 3 years.

IVUS RESULTS

IVUS measurements were available in 28 (100%) patients at 6 months, 17 (100%) patients at 1 year, 21 (75.0%) patients at 2 years, and 8 (47.1%) patients at 3 years. As shown in **Table 3** and **Supplementary Figure 6**, the mean vessel, scaffold and lumen areas were stable between 6-month and 24-month follow-up but were larger at 36 months. The minimum lumen and scaffold areas

Table 2. Quantitative coronary angiographic serial assessments.

		Post-procedure (all patients, n=45)	6 months (cohort 1, n=28)	1 year (cohort 2, n=17)	2 years (cohort 1, n=21)	3 years (cohort 2, n=8)	*p*-value post-procedure vs 6 months	*p*-value 6 months vs 1 year	*p*-value 1 year vs 2 years	*p*-value 2 years vs 3 years
RVD, mm	In-scaffold	3.08±0.39	3.00±0.33	2.93±0.38	3.04±0.36	3.00±0.35	0.33	0.52	0.34	0.78
	In-segment	3.00±0.44	2.96±0.35	2.87±0.41	3.06±0.47	2.87±0.43	0.71	0.41	0.18	0.32
MLD, mm	In-scaffold	2.78±0.36	2.46±0.44	2.37±0.58	2.39±0.44	2.51±0.46	0.001	0.56	0.90	0.54
	In-segment	2.55±0.39	2.35±0.40	2.20±0.50	2.34±0.41	2.36±0.41	0.03	0.28	0.36	0.89
DS, %	In-scaffold	9.3±6.5	17.5±12.6	18.1±18.6	21.2±10.8	16.0±15.1	0.003	0.91	0.55	0.30
	In-segment	14.3±7.3	20.3±10.9	22.1±17.9	23.1±10.9	16.8±15.1	0.014	0.72	0.84	0.21
Binary restenosis	In-scaffold	-	1 (3.6%)	2 (11.8%)	1 (4.5%)	0 (0%)	-	0.55	0.57	1.00
	In-segment	-	1 (3.6%)	2 (11.8%)	1 (4.5%)	0 (0%)	-	0.55	0.57	1.00
LLL, mm	In-scaffold	-	0.33±0.27	0.39±0.50	0.40±0.31	0.37±0.57	-	0.63	0.95	0.86
	In-segment	-	0.25±0.26	0.27±0.45	0.27±0.35	0.21±0.38	-	0.88	0.99	0.67
Vasomotion, mm		-	0.11±0.12	0.15±0.28	0.13±0.10	0.10±0.15	-	0.62	0.80	0.54
Quantitative flow ratio		0.95±0.03	0.93±0.07	0.87±0.13	0.95±0.03	0.88±0.08	0.15	0.10	0.04	0.07

Data are mean±standard deviation or number (%). DS: diameter stenosis; LLL: late lumen loss; MLD: minimum lumen diameter; RVD: reference vessel diameter

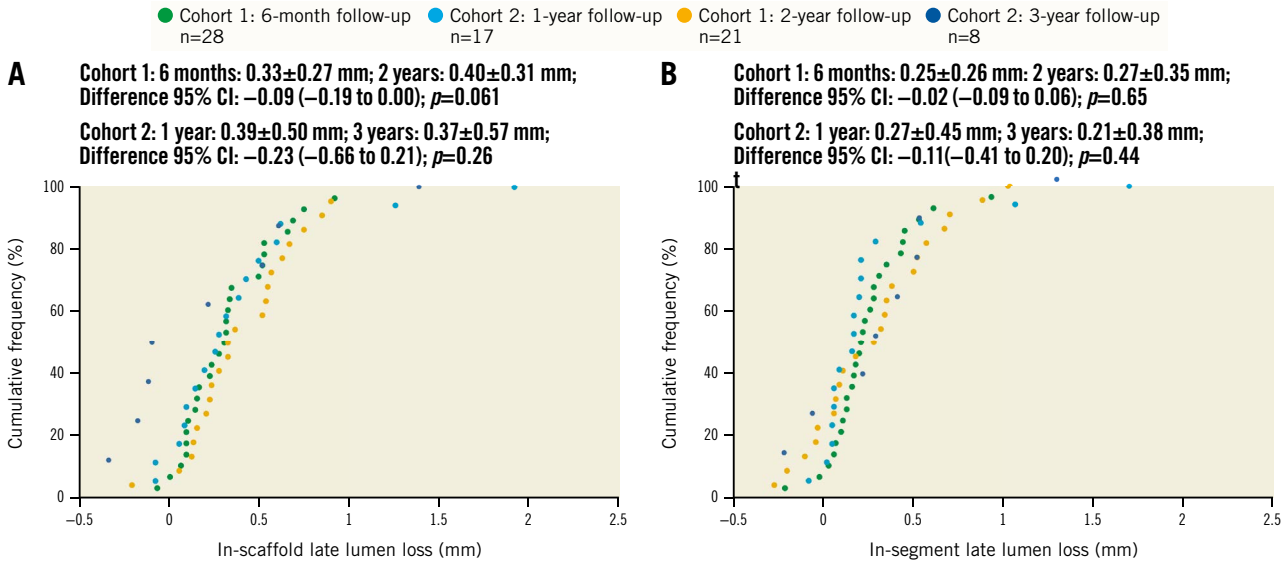

Figure 1. *Cumulative frequency of in-scaffold and in-segment late lumen loss up to 3 years by quantitative coronary angiography. A) In-scaffold late lumen loss. B) In-segment late lumen loss. Paired difference calculated in 21 patients in cohort 1 and 8 patients in cohort 2. CI: confidence interval*

Table 3. Intravascular ultrasound serial assessments.

	Post-procedure (all patients, n=45)	6 months (cohort 1, n=28)	1 year (cohort 2, n=17)	2 years (cohort 1, n=21)	3 years (cohort 2, n=8)	*p*-value post-procedure vs 6 months	*p*-value 6 months vs 1 year	*p*-value 1 year vs 2 years	*p*-value 2 years vs 3 years
Mean vessel area, mm²	17.4±3.5	17.3±3.5	17.5±3.6	17.4±3.6	20.4±4.0	0.88	0.82	0.95	0.07
Min vessel area, mm²	14.3±3.3	14.0±2.8	13.6±3.1	13.5±2.7	15.6±3.4	0.71	0.68	0.87	0.08
Mean lumen area, mm²	9.21±1.79	7.76±2.00	7.70±2.15	7.61±2.08	8.62±2.29	0.002	0.91	0.91	0.27
Min lumen area, mm²	7.67±1.50	5.62±1.74	5.43±1.91	5.09±1.28	5.73±1.35	<0.0001	0.74	0.51	0.24
Mean plaque area, mm²	8.19±2.37	9.51±2.32	9.82±2.35	9.83±1.95	11.77±2.54	0.02	0.66	1.00	0.04
Mean scaffold area, mm²	9.30±1.80	8.72±1.96	8.91±1.97	9.00±2.09	10.5±2.75	0.20	0.75	0.90	0.12
Min scaffold area, mm²	7.77±1.51	6.93±1.54	6.75±1.42	6.39±1.38	7.82±2.20	0.02	0.71	0.43	0.04
NHA, mm²	-	0.77±0.45	1.09±0.90	1.17±0.87	1.75±0.77	-	0.18	0.79	0.11
Area obstruction, %	-	11.8±5.7	14.7±10.3	15.9±9.1	18.3±5.21	-	0.31	0.70	0.48
Volumetric obstruction*, %	-	11.7±5.8	14.7±10.4	15.7±8.9	17.8±5.22	-	0.29	0.76	0.53
Mean recoil area, mm²	-	0.67±0.90	0.23±1.08	0.46±1.91	−0.88±2.63	-	0.15	0.64	0.14
Recoil area, %	-	7.0±10.0	2.7±13.0	3.3±20.7	−10.2±27.0	-	0.22	0.92	0.16

Data are mean±standard deviation. *In-scaffold. Min: minimum; NHA: neointimal hyperplasia area

progressively decreased up to 2 years but were larger at 3 years, while the degree of neointimal hyperplasia increased up to 3-year follow-up. The mean scaffold area recoil was 7% at 6 months, 3% at 1 year and 2 years, and −10.2% at 3 years (indicating expansion). Paired analyses showed that the minimum vessel area was significantly reduced from 6 months to 2 years in cohort 1, while plaque area was significantly increased from 1 year to 3 years in cohort 2 **(Supplementary Table 4)**. The proportion of struts categorised as showing obvious absorption were 7.4%, 35.7%, 59.8% and 78.1% at 6 months, 1 year, 2 years and 3 years, respectively **(Supplementary Figure 3)**.

OCT RESULTS

OCT measurements were available in 28 (100%) patients at 6 months, 17 (100%) patients at 1 year, 21 (75.0%) patients at 2 years, and 8 (47.1%) patients at 3 years. As shown in **Table 4** and **Figure 2**, the mean scaffold area did not change from post-procedure to 2 years but was larger at 3 years. The mean lumen area reached its nadir at 6 months, while the minimum scaffold and lumen areas decreased up to 2-year follow-up and then increased at 3 years. The neointimal area and percentage area obstruction peaked at 6 months and were unchanged up to 2 years; the neointimal area then increased at 3 years. Paired analyses showed similar

Table 4. Optical coherence tomography serial assessments.

	Post-procedure	6 months	1 year	2 years	3 years	*p*-value post-procedure vs 6 months	*p*-value 6 months vs 1 year	*p*-value 1 year vs 2 years	*p*-value 2 years vs 3 years
Strut level	n=20,917	n=12,122	n=7,072	n=8,299	n=3,231				
Strut coverage thickness, µm	-	194.1±140.1	185.6±139.3	183.0±107.1	279.7±148.5	-	<0.0001	0.17	<0.0001
ISA	224 (1.1)	6 (0.05)	1 (0.01)	0 (0)	0 (0)	<0.0001	0.44	0.46	0.28
Late-acquired ISA	-	0 (0)	0 (0)	0 (0)	0 (0)	-	-	-	-
Cross-section level	n=2,239	n=1,372	n=851	n=1,062	n=416				
Neointimal area, mm^2	-	1.67±0.93	1.67±1.08	1.58±0.74	2.75±1.22	-	0.91	0.03	<0.0001
Covered struts	-	1,369 (99.8)	851 (100)	1,062 (100)	416 (100)	-	0.29	NA	0.28
Lesion level	n=44	n=28	n=17	n=21	n=8				
Mean scaffold area, mm^2	8.92±1.79	8.83±2.13	9.07±2.04	9.15±2.28	10.74±2.86	0.85	0.71	0.91	0.13
Minimum scaffold area, mm^2	7.37±1.55	7.04±1.80	7.12±1.65	5.99±1.41	7.51±2.13	0.41	0.88	0.03	0.03
Mean scaffold diameter, mm	3.35±0.34	3.32±0.42	3.37±0.38	3.37±0.42	3.66±0.48	0.77	0.69	0.99	0.13
Minimum scaffold diameter, mm	3.13±0.34	3.11±0.40	3.13±0.38	3.10±0.38	3.39±0.43	0.83	0.87	0.81	0.09
Mean luminal area, mm^2	8.71±1.78	7.22±2.26	7.44±2.34	7.62±2.40	8.03±2.32	0.003	0.76	0.81	0.68
Minimum luminal area, mm^2	7.11±1.53	4.81±2.21	5.22±2.16	4.43±1.53	4.55±1.59	<0.0001	0.55	0.20	0.86
Area obstruction, %	18.2±6.3	19.9±8.9	19.5±11.9	18.1±7.9	25.4±6.46	0.38	0.88	0.67	0.03
Healing score*	197.8±5.7	0.1±0.4	0.01±0.1	0.0±0.0	0.0±0.0	<0.0001	0.24	0.33	0.35
Absolute late recoil, mm^2	-	0.25±1.24	–0.32±1.18	–0.09±1.73	–1.20±2.48	-	0.14	0.65	0.19
Late recoil, %	-	2.9±14.5	–4.2±14.2	–1.3±19.2	–13.4±26.0	-	0.12	0.61	0.18
Absorption, %	-	34.3±11.1	52.3±11.9	82.3±10.0	95.4±3.8	-	<0.0001	<0.0001	<0.0001

Data are mean±standard deviation or number (%). *Healing score = (presence of intra-scaffold structure × 4) + (presence of both malapposed and uncovered struts × 3) + (presence of uncovered struts alone × 2) + (presence of malapposition alone × 1). ISA: incomplete strut apposition

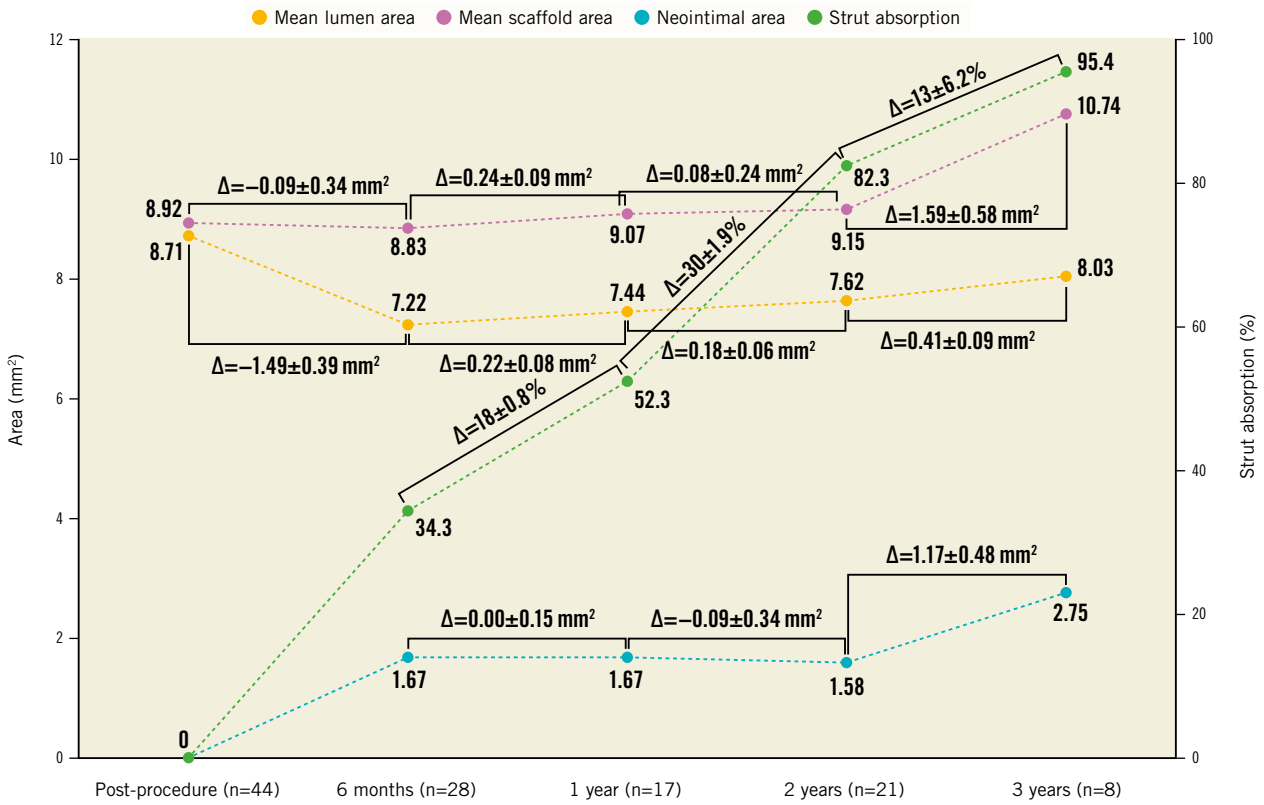

Figure 2. *Serial OCT assessments up to 3-year follow-up. The orange line illustrates mean lumen area changes; the purple line illustrates mean scaffold area changes; the blue line illustrates neointimal area changes; the green line illustrates percentage of strut absorption changes.*

results **(Supplementary Table 5)**. In the patient who required bail-out IBS treatment for an edge dissection, 6-month and 2-year follow-up angiography showed that the overlap region was well covered with tissue and that the lumen was patent without thrombosis **(Supplementary Figure 7)**. The lumen and scaffold area evolution by OCT in the 4 patients who underwent TLR are shown in **Supplementary Figure 8**. Incomplete strut apposition was infrequent at all time periods, and late-acquired strut malapposition was not observed. The proportion of covered struts was 99.8% at 6 months and 100% at 1-year, 2-year and 3-year follow-up. The strut absorption rate was 34.3% at 6 months, 52.3% at 1 year, 82.3% at 2 years and 95.4% at 3 years **(Supplementary Figure 9, Supplementary Figure 10)**.

Discussion

The major findings from this first-in-human study, in which the outcomes of a novel ultrathin-strut sirolimus-eluting IBS were evaluated up to 3 years with clinical and multimodality imaging, are as follows: 1) coronary implantation of the IBS was feasible in non-complex lesions, with 100% device, lesion and procedural success; 2) long-term safety and effectiveness in these non-complex lesions were demonstrated, with a 6.7% 3-year TLF rate, all due to CI-TLR, with no deaths, MIs or scaffold thromboses; 3) the QCA in-scaffold LLL up to 3 years was acceptable (mean 0.37 mm), with only 3 cases (6.7%) of in-segment binary restenosis; 4) strut coverage was rapid, and no strut fractures or late-acquired malapposition were observed; and 5) the rate of strut resorption steadily increased from 34.3% at 6 months to 95.4% at 3 years, without malapposition during the bioresorption process **(Central illustration)**.

The present study is the first report of a novel IBS coronary artery implanted in a human. The iron content in a 3.0x18 mm IBS is 9 mg, which is equivalent to that in approximately 20 ml of blood or the weekly iron intake of an adult. Thus, IBS scaffold implantation should not induce iron overload. Compared with most bioabsorbable polymeric scaffolds, the strut thickness of the IBS is substantially less and the resorption rate is faster[23]. The thin iron struts may result in better tissue embedding and more rapid endothelialisation, which may prevent acute and acquired malapposition and late scaffold intraluminal dismantling[23]. Indeed, by OCT 99.8% and 100% of all struts were covered by 6 months and 12 months, respectively, and no cases of late malapposition of scaffold discontinuities were observed. It is possible that this rapid endothelialsation rate would enable shortening DAPT to 6 months, a hypothesis that requires testing in future studies. The scaffold also provided acceptable acute radial strength, and recoil up to 3 years was minimal. Angiographic vasoreactivity was evidenced as soon as 6 months after implantation and was stable over time.

As measured by QCA, the mean 0.33 mm in-scaffold LLL of the IBS at 6 months is higher than that of contemporary permanent

EuroIntervention

CENTRAL **ILLUSTRATION** Clinical performance of the novel ultrathin sirolimus-eluting iron bioresorbable scaffold

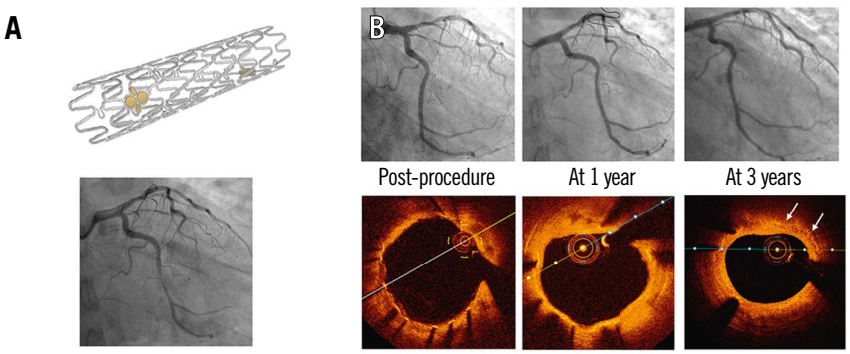

C

Imaging assessment	Post-procedure	6 months	1 year	2 years	3 years
Target lesion failure	-	1 (2.2%)	3 (6.7%)	3 (6.7%)	3 (6.7%)
In-scaffold late lumen lumen loss by QCA, mm	-	0.33±0.27	0.39±0.50	0.40±0.31	0.37±0.57
Mean scaffold area by IVUS, mm^2	9.30±1.80	8.72±1.96	8.91±1.97	9.00±2.09	10.50±2.75
Proportion of covered struts by OCT, %	-	1,369 (99.8%)	851 (100%)	1,062 (100%)	416 (100%)
Absorption by OCT, %	-	34.3±11.1	52.3±11.9	82.3±10.0	95.4±3.8

The iron bioresorbable scaffold (A), a representative case with angiographic and OCT follow-up at 1 and 3 years (B), and selected study results from the first-in-human experience in its implant in 45 patients with a single non-complex coronary artery lesion (C).
IVUS: intravascular ultrasound; OCT: optical coherence tomography; QCA: quantitative coronary angiography

metallic DES, such as EES (0.17 mm)[24] and some polymeric BRS[23], such as the Absorb BVS (0.16 mm)[25] and DESolve (Elixir Medical; 0.20 mm)[21], but lower than the third-generation magnesium BRS Magmaris (BIOTRONIK; 0.44 mm)[11]. However, the in-scaffold LLL of permanent DES and most polymeric and magnesium-based BRS continue to increase up to 3 years (ranging from 0.27 to 0.54 mm)[11,24-26], similar to that of the IBS. Moreover, there was no significant increase in the IBS in-segment LLL up to 3 years, consistent with the constancy of the mean thickness of strut coverage and in-scaffold volumetric obstruction measured by OCT and IVUS during this period.

In the present study, we utilised a novel OCT-based semiquantitative method to analyse the IBS absorption process, based on experimental observations[15]. The zinc buffer layer on the scaffold backbone was specifically designed to prevent the IBS from degradation within 3 months after implantation. Thus, assuming minimal bioresorption within the first 3 months, it may be estimated that the absorption rate during follow-up was approximately 11.4% per month from 3 to 6 months, 3% per month from 6 months to 1 year, 2.5% per month from 1 to 2 years, and 1.1% per month from 2 to 3 years. Despite the ongoing absorption process up to 3 years, the mean lumen area, scaffold area and extent of neointimal hyperplasia were stable during this period. The mean scaffold area measured by OCT and IVUS showed no significant reduction from post-procedure to 3 years, indicating sufficient radial force of the scaffold to maintain its geometrical shape during the bioresorption process. The mean luminal area decreases from post-procedure to 6 months were mainly due to neointimal proliferation, while compensatory expansive remodelling was observed from 2 years to 3 years as observed in previous BRS studies[1,27,28]. However, in selected cases the strut bioresorption rate may be too fast, resulting in early scaffold collapse, as seen in the second TLR case. To prevent such early strut biocorrosion, the IBS processing may be further improved by tightening control of the minimum thickness of the zinc layer and the maximum thickness of the polymer coating.

Compared to the other currently available bioabsorbable metal scaffold, the magnesium-based Magmaris, the IBS is thinner (70 μm vs 150 μm), and the Magmaris completely resorbs within 12 months, as compared with >3 years with the IBS, as demonstrated in the present study[17,29]. The mean 6-month QCA in-scaffold LLL of the IBS from the present study (0.33 mm) was slightly less than that with the Magmaris (0.44 mm)[11]. In the BIOSOLVE-IV study, the 12-month TLF rate with the second-generation Magmaris (the DREAMS 2G) scaffold in 1,075 patients was low (4.3%, including 0.2% cardiac death, 1.1% TV-MI, and 3.9% TLR), with 0.5% definite or probable device thrombosis, and all events occurred between 6 and 95 days after PCI[29]. While the absence of any deaths, MIs or scaffold thromboses up to 3 years with the IBS is promising, the sample size is too small to draw meaningful comparisons. Moreover, a new third-generation Magmaris (DREAMS 3G) has reported even lower 6-month in-scaffold LLL (0.21 mm) and TLF rate at 6 months (0.9%) (Haude M. Safety and Clinical Performance of the Sirolimus Eluting Resorbable Coronary Magnesium Scaffold System [DREAMS 3G] in the Treatment of Subjects With *De Novo* Lesions in Native Coronary Arteries - BIOMAG-I First-In-Human Trial. TCT 2022, Boston, MA, USA); longer-term follow-up results are warranted with this device to enable comparison with the IBS in comparable patients.

Limitations

There are limitations to the present study. First, this was a small, single-arm, first-in-human study, with the results reflecting the performance of the IBS in a highly selected, non-complex patient and lesion population, which may have contributed to the low rate of observed TLR. Second, the absence of a concurrent control arm limits the interpretation of our results. Third, additional OCT analyses are needed to assess the properties of this novel device. In particular, the OCT semiquantitative method proposed in the present study to evaluate the rate of bioabsorption warrants further evaluation. Finally, the results are complete up to 3-year follow-up; longer-term clinical and imaging follow-up is warranted to evaluate the safety and efficacy of this new device.

Conclusions

In conclusion, the 3-year clinical outcomes and serial multimodality imaging assessments of the novel IBS have demonstrated the feasibility and potential safety and effectiveness of this device for the treatment of patients with non-complex coronary artery lesions.

Impact on daily practice

Three-year clinical follow-up results and serial multimodality imaging assessments of the novel IBS – an ultrathin (70 μm) sirolimus-eluting iron bioresorbable coronary scaffold consisting of a 53 μm nitriding iron backbone with a pure zinc submicron layer – in the treatment of patients with non-complex coronary lesions documented its feasibility and preliminary safety and efficacy. Late lumen loss was acceptable (mean 0.33 mm at 6 months and 0.37 mm at 3 years), and by 3 years the scaffold was 95.4% absorbed. A randomised trial with adequate statistical power is warranted to assess the clinical performance of IBS compared with contemporary metallic drug-eluting stents in patients with coronary artery disease.

Acknowledgements

The authors are grateful to the participating patients for their contributions to the trial. We also thank all the physicians and nurses who cared for these patients and all the clinical and research staff who assisted in the study.

Funding

The IBS-FIM trial was funded by Biotyx Medical, Shenzhen, People's Republic of China. Biotyx Medical was involved in the study design, monitoring and data collection. The corresponding author directed the study, had full access to all the data and final responsibility for the data interpretation and decision to submit for publication. The funder had the right to a non-binding review of the manuscript.

Conflict of interest statement

R. Gao has received institutional research grants from Biotyx Medical. G.W. Stone has received speaker honoraria from Medtronic, Pulnovo, Infraredx, and Abiomed; has served as a consultant to Valfix, TherOx, Robocath, HeartFlow, Ablative Solutions, Vectorious, Miracor Medical, Neovasc, Ancora, Elucid Bio, Occlutech, CorFlow, Apollo Therapeutics, Impulse Dynamics, CardioMech, Gore, Amgen, Adona Medical, and Millennia Biopharma; and has equity/options in Ancora, Cagent, Applied Therapeutics, BioStar family of funds, SpectraWAVE, Orchestra BioMed, Aria, Cardiac Success, Valfix, and Xenter. G.W. Stone's daughter is an employee at IQVIA. G.W. Stone's employer, Mount Sinai Hospital, receives research support from Abbott, Abiomed, Bioventrix, Cardiovascular Systems, Inc., Philips, Biosense Webster, Inc., Shockwave Medical, Vascular Dynamics, Pulnovo Medical, and V-Wave Ltd. The other authors have no conflicts of interest to declare.

References

1.Serruys PW, Ormiston JA, Onuma Y, Regar E, Gonzalo N, Garcia-Garcia HM, Nieman K, Bruining N, Dorange C, Miquel-Hébert K, Veldhof S, Webster M, Thuesen L, Dudek D. A bioabsorbable everolimus-eluting coronary stent system (ABSORB): 2-year outcomes and results from multiple imaging methods. *Lancet.* 2009;373:897-910.

2. Katagiri Y, Stone GW, Onuma Y, Serruys PW. State of the art: the inception, advent and future of fully bioresorbable scaffolds. *EuroIntervention.* 2017;13:734-50.

3. Haude M, Erbel R, Erne P, Verheye S, Degen H, Böse D, Vermeersch P, Wijnbergen I, Weissman N, Prati F, Waksman R, Koolen J. Safety and performance of the drug-eluting absorbable metal scaffold (DREAMS) in patients with de-novo coronary lesions: 12 month results of the prospective, multicentre, first-in-man BIOSOLVE-I trial. *Lancet.* 2013;381:836-44.

4. Kereiakes DJ, Ellis SG, Metzger DC, Caputo RP, Rizik DG, Teirstein PS, Litt MR, Kini A, Kabour A, Marx SO, Popma JJ, Tan SH, Ediebah DE, Simonton C, Stone GW; ABSORB III Investigators. Clinical Outcomes Before and After Complete Everolimus-Eluting Bioresorbable Scaffold Resorption: Five-Year Follow-Up From the ABSORB III Trial. *Circulation.* 2019;140:1895-903.

5. Kozuma K, Tanabe K, Hamazaki Y, Okamura T, Ando J, Ikari Y, Nakagawa Y, Kusano H, Ediebah D, Kimura T; ABSORB Japan Investigators. Long-Term Outcomes of Absorb Bioresorbable Vascular Scaffold vs. Everolimus-Eluting Metallic Stent - A Randomized Comparison Through 5 Years in Japan. *Circ J.* 2020;84:733-41.

6. Stone GW, Kimura T, Gao R, Kereiakes DJ, Ellis SG, Onuma Y, Chevalier B, Simonton C, Dressler O, Crowley A, Ali ZA, Serruys PW. Time-Varying Outcomes With the Absorb Bioresorbable Vascular Scaffold During 5-year Follow-up: A Systematic Meta-analysis and Individual Patient Data Pooled Study. *JAMA Cardiol.* 2019;4:1261-9.

7. Yamaji K, Ueki Y, Souteyrand G, Daemen J, Wiebe J, Nef H, Adriaenssens T, Loh JP, Lattuca B, Wykrzykowska JJ, Gomez-Lara J, Timmers L, Motreff P, Hoppmann P, Abdel-Wahab M, Byrne RA, Meincke F, Boeder N, Honton B, O'Sullivan CJ, Ielasi A, Delarche N, Christ G, Lee JKT, Lee M, Amabile N, Karagiannis A, Windecker S, Räber L. Mechanisms of Very Late Bioresorbable Scaffold Thrombosis: The INVEST Registry. *J Am Coll Cardiol.* 2017;70:2330-44.

8. Peng X, Qu W, Jia Y, Wang Y, Yu B, Tian J. Bioresorbable Scaffolds: Contemporary Status and Future Directions. *Front Cardiovasc Med.* 2020;7:589571.

9. Erbel R, Di Mario C, Bartunek J, Bonnier J, de Bruyne B, Eberli FR, Erne P, Haude M, Heublein B, Horrigan M, Ilsley C, Böse D, Koolen J, Lüscher TF, Weissman N, Waksman R; PROGRESS-AMS (Clinical Performance and Angiographic Results of Coronary Stenting with Absorbable Metal Stents) Investigators. Temporary scaffolding of coronary arteries with bioabsorbable magnesium stents: a prospective, non-randomised multicentre trial. *Lancet.* 2007;369:1869-75.

10. Cubero-Gallego H, Vandeloo B, Gomez-Lara J, Romaguera R, Roura G, Gomez-Hospital JA, Cequier A. Early Collapse of a Magnesium Bioresorbable Scaffold. *JACC Cardiovasc Interv.* 2017;10:e171-2.

11. Haude M, Ince H, Toelg R, Lemos PA, von Birgelen C, Christiansen EH, Wijns W, Neumann FJ, Eeckhout E, Garcia-Garcia HM, Waksman R. Safety and performance of the second-generation drug-eluting absorbable metal scaffold (DREAMS 2G) in patients with de novo coronary lesions: three-year clinical results and angiographic findings of the BIOSOLVE-II first-in-man trial. *EuroIntervention.* 2020;15:e1375-82.

12. Peuster M, Wohlsein P, Brügmann M, Ehlerding M, Seidler K, Fink C, Brauer H, Fischer A, Hausdorf G. A novel approach to temporary stenting: degradable cardiovascular stents produced from corrodible metal-results 6-18 months after implantation into New Zealand white rabbits. *Heart.* 2001;86:563-9.

13. Waksman R, Pakala R, Baffour R, Seabron R, Hellinga D, Tio FO. Short-term effects of biocorrodible iron stents in porcine coronary arteries. *J Interv Cardiol.* 2008;21:15-20.

14. Wu C, Qiu H, Hu XY, Ruan YM, Tian Y, Chu Y, Xu XL, Xu L, Tang Y, Gao RL. Short-term safety and efficacy of the biodegradable iron stent in mini-swine coronary arteries. *Chin Med J (Engl).* 2013;126:4752-7.

15. Lin W, Qin L, Qi H, Zhang D, Zhang G, Gao R, Qiu H, Xia Y, Cao P, Wang X, Zheng W. Long-term in vivo corrosion behavior, biocompatibility and bioresorption mechanism of a bioresorbable nitrided iron scaffold. *Acta Biomater.* 2017;54:454-68.

16. Zhang H, Zhang W, Qiu H, Zhang G, Li X, Qi H, Guo J, Qian J, Shi X, Gao X, Shi D, Zhang D, Gao R, Ding J. A Biodegradable Metal-Polymer Composite Stent Safe and Effective on Physiological and Serum-Containing Biomimetic Conditions. *Adv Healthc Mater.* 2022:e2201740.

17. Lin W-J, Zhang D-Y, Zhang G, Sun H-T, Qi H-P, Chen L-P, Liu Z-Q, Gao R-L, Zheng W. Design and characterization of a novel biocorrodible iron-based drug-eluting coronary scaffold. *Materials and Design.* 2016;91:72-9.

18. Shen D, Qi H, Lin W, Zhang W, Bian D, Shi X, Qin L, Zhang G, Fu W, Dou K, Xu B, Yin Z, Rao J, Alwi M, Wang S, Zheng Y, Zhang D, Gao R. PDLLA-Zn-nitrided Fe bioresorbable scaffold with 53-μm-thick metallic struts and tunable multistage biodegradation function. *Sci Adv.* 2021;7:eabf0614.

19. Zheng JF, Qiu H, Tian Y, Hu XY, Luo T, Wu C, Tian Y, Tang Y, Song LF, Li L, Xu L, Xu B, Gao RL. Preclinical Evaluation of a Novel Sirolimus-Eluting Iron Bioresorbable Coronary Scaffold in Porcine Coronary Artery at 6 Months. *JACC Cardiovasc Interv.* 2019;12:245-55.

20. Garcia-Garcia HM, Serruys PW, Campos CM, Muramatsu T, Nakatani S, Zhang YJ, Onuma Y, Stone GW. Assessing bioresorbable coronary devices: methods and parameters. *JACC Cardiovasc Imaging.* 2014;7:1130-48.

21. Abizaid A, Costa RA, Schofer J, Ormiston J, Maeng M, Witzenbichler B, Botelho RV, Costa JR Jr, Chamié D, Abizaid AS, Castro JP, Morrison L, Toyloy S, Bhat V, Yan J, Verheye S. Serial Multimodality Imaging and 2-Year Clinical Outcomes of the Novel DESolve Novolimus-Eluting Bioresorbable Coronary Scaffold System for the Treatment of Single De Novo Coronary Lesions. *JACC Cardiovasc Interv.* 2016;9:565-74.

22. Lin W, Zhang H, Zhang W, Qi H, Zhang G, Qian J, Li X, Qin L, Li H, Wang X, Qiu H, Shi X, Zheng W, Zhang D, Gao R, Ding J. In vivo degradation and endothelialization of an iron bioresorbable scaffold. *Bioact Mater.* 2021;6:1028-39.

23. Regazzoli D, Leone PP, Colombo A, Latib A. New generation bioresorbable scaffold technologies: an update on novel devices and clinical results. *J Thorac Dis.* 2017;9:S970-85.

24. Claessen BE, Beijk MA, Legrand V, Ruzyllo W, Manari A, Varenne O, Suttorp MJ, Tijssen JG, Miquel-Hebert K, Veldhof S, Henriques JP, Serruys PW, Piek JJ. Two-year clinical, angiographic, and intravascular ultrasound follow-up of the XIENCE V everolimus-eluting stent in the treatment of patients with de novo native coronary artery lesions: the SPIRIT II trial. *Circ Cardiovasc Interv.* 2009;2:339-47.

25. Ormiston JA, Serruys PW, Onuma Y, van Geuns RJ, de Bruyne B, Dudek D, Thuesen L, Smits PC, Chevalier B, McClean D, Koolen J, Windecker S, Whitbourn R, Meredith I, Dorange C, Veldhof S, Hebert KM, Rapoza R, Garcia-Garcia HM. First serial assessment at 6 months and 2 years of the second generation of absorb everolimus-eluting bioresorbable vascular scaffold: a multi-imaging modality study. *Circ Cardiovasc Interv.* 2012;5:620-32.

26. Hermiller JB, Nikolsky E, Lansky AJ, Applegate RJ, Sanz M, Yaqub M, Sood P, Cao S, Sudhir K, Stone GW. Clinical and angiographic outcomes of elderly patients treated with everolimus-eluting versus paclitaxel-eluting stents: three-year results from the SPIRIT III randomised trial. *EuroIntervention.* 2011;7:307-13.

27. Nakatani S, Ishibashi Y, Sotomi Y, Perkins L, Eggermont J, Grundeken MJ, Dijkstra J, Rapoza R, Virmani R, Serruys PW, Onuma Y. Bioresorption and Vessel Wall Integration of a Fully Bioresorbable Polymeric Everolimus-Eluting Scaffold: Optical Coherence Tomography, Intravascular Ultrasound, and Histological Study in a Porcine Model With 4-Year Follow-Up. *JACC Cardiovasc Interv.* 2016;9:838-51.

28. Serruys PW, Katagiri Y, Sotomi Y, Zeng Y, Chevalier B, van der Schaaf RJ, Baumbach A, Smits P, van Mieghem NM, Bartorelli A, Barragan P, Gershlick A, Kornowski R, Macaya C, Ormiston J, Hill J, Lang IM, Egred M, Fajadet J, Lesiak M, Windecker S, Byrne RA, Räber L, van Geuns RJ, Mintz GS, Onuma Y. Arterial Remodeling After Bioresorbable Scaffolds and Metallic Stents. *J Am Coll Cardiol.* 2017;70:60-74.

29. Verheye S, Wlodarczak A, Montorsi P, Torzewski J, Bennett J, Haude M, Starmer G, Buck T, Wiemer M, Nuruddin AAB, Yan BP, Lee MK. BIOSOLVE-IV-registry: Safety and performance of the Magmaris scaffold: 12-month outcomes of the first cohort of 1,075 patients. *Catheter Cardiovasc Interv.* 2021;98:E1–8.

Supplementary data

Supplementary Appendix 1. Inclusion and exclusion criteria.

Supplementary Appendix 2. Definitions of the prespecified endpoints.

Supplementary Appendix 3. Cases of TLR and TVR.

Supplementary Table 1. Baseline characteristics and procedural results.

Supplementary Table 2. Medications at discharge and up to 3-year follow-up.

Supplementary Table 3. Paired quantitative coronary angiography results in cohort 1 and cohort 2.

Supplementary Table 4. Paired intravascular ultrasound analysed results in cohort 1 and cohort 2.

Supplementary Table 5. Paired optical coherence tomography analysed results in cohort 1 and cohort 2.

Supplementary Figure 1. Device description.

Supplementary Figure 2. Experimental animal results.

Supplementary Figure 3. Scaffold absorption as assessed by IVUS.

Supplementary Figure 4. Scaffold absorption as assessed by OCT.

Supplementary Figure 5. Study flowchart.

Supplementary Figure 6. Serial IVUS assessments up to 3-year follow-up.

Supplementary Figure 7. Six-month and two-year imaging follow-up of a patient with the bailout IBS.

Supplementary Figure 8. OCT assessment in four cases undergoing target lesion revascularisation.

Supplementary Figure 9. Scaffold absorption assessed by OCT.

Supplementary Figure 10. Scaffold absorption assessed by OCT (paired measurements).

The supplementary data are published online at: https://eurointervention.pcronline.com/doi/10.4244/EIJ-D-22-00919

Supplementary data

Supplementary Appendix 1. Inclusion and exclusion criteria.

1.1 Inclusion criteria:

All patients participating in this clinical trial must meet the following criteria:

1. Age of 18-75, males or non-pregnant females;
2. Subject must have evidence of myocardial ischemia (e.g., stable, unstable angina, post-infarct angina or silent ischemia) suitable for elective PCI;
3. One target lesion, and target lesion can be completely covered by a single stent;
4. Target lesion length ⩽ 18 mm, target lesion diameter between 3.0 mm to 3.5 mm (visual);
5. Visual assessment of target lesion stenosis ⩾70%, TIMI blood flow⩾ 1;
6. Subject who understands the purpose of testing, voluntary and informed consent, patients undergoing invasive imaging follow-up.

1.2 Exclusion criteria:

Patients will be excluded if any of the following conditions apply:

General:

1. Within 1 week of any acute myocardial infarction or levels of myocardial enzymes did not return to normal;
2. Implantation of stent in target vessel within 1 year , patients with planned intervention again within six months;
3. Patients who underwent coronary artery bypass (coronary artery bypass grafting);
4. Patients with contraindications for coronary artery bypass graft surgery;
5. Severe heart failure (NYHA class III and above) or left ventricular ejection fraction<40% (ultrasonic or left ventricular angiography);
6. Preoperative renal function: serum creatinine > 2.0 mg/dl or 177 μmol/L; receiving hemodialysis;
7. Patients had ischemic stroke half a year before implantation, patients had transient ischemic attack 3 months before implantation, patients have high coagulation tendency judged by investigator or laboratory examination;
8. Bleeding, active gastrointestinal ulcers, brain hemorrhage or subarachnoid hemorrhage, contraindications on antiplatelet agents and anticoagulant therapy; patients would not allow receiving antithrombotic therapy;
9. Aspirin, clopidogrel, heparin, contrast agent, poly lactic acid polymer, rapamycin and metal allergies;
10. Patients who have a history of disease related to iron overload or iron disorder, such as hereditary hemochromatosis, among others;
11. The patient's life expectancy is less than 12 months;
12. Patient participates in other drug or medical device study and does not meet the primary study endpoint in clinical trials time frame;

13. Poor compliance and patients unable to complete the study in accordance with the requirements;
14. Patient with heart transplant;
15. Unstable arrhythmia, such as high risk ventricular extra systole and ventricular tachycardia;
16. Cancer needing chemotherapy;
17. Patients with immune suppression, autoimmune diseases, planned or undergoing immunosuppressive therapy;
18. Planning or receiving long-term anticoagulant therapy, such as heparin, warfarin, among others;
19. Within six months of elective surgery requiring discontinuation of aspirin and clopidogrel;
20. Blood test showing platelet count $< 100 \times 10^9$/L, or $> 700 \times 10^9$/L, white blood cells $< 3 \times 10^9$/L, or abnormal liver function (ALT, AST 3 times greater than normal range);
21. Patients with diffuse peripheral vascular disease; cannot use 6F catheter;
22. Patients with valvular surgery in the past.

Exclusion criteria by angiography:

1. Chronic total occlusion (TIMI blood flow=0 before implantation) , left main coronary artery lesion, ostial lesion, multiple vessel lesion, branch lesion and bridge lesion with branch vessel diameter ≥ 2.0 mm (if the ostium of branch vessel stenosis >40% or needs balloon predilation); visible thrombus in target vessels;
2. Severe calcified lesions and distorted disease which is amenable toto predilation, lesion not suitable for stent delivery and expansion;
3. In-stent restenosis;
4. Myocardial bridge is involved in target lesion;
5. To reach the target lesion, study stent has to go through a previously implanted stent;
6. Predilation balloon cannot expand completely in target lesion site, judgment standard for full expansion as below, patients are excluded when do not meet any item:
    1. DS% < 40%(visual), highly recommend DS% ≤20%
    2. TIMI blood flow= class 3 (visual)
    3. No angiography complications (e.g., distal embolization, lateral branch closed)
    4. No interlining level NHLBI type D - F
    5. No continuous chest pain (> 5 minutes), and
    6. No lower or higher ST segment >5 minutes.

1.3 Bail-out stenting

The studied IBS was the first choice once a bail-out device was needed for complications, if the device size was not suitable, Xience (Abbott Vascular) was allowed to be used as bail-out stent.

Supplementary Appendix 2. Definitions of the prespecified endpoints.

2.1 Acute success

Device success (device level analysis): defined as successful delivery and deployment of the study scaffold at the intended target lesion and successful withdrawal of the delivery system with attainment of final in-scaffold residual stenosis of <30% by visual estimation and TIMI Grade-3 flow.

Lesion success (lesion level analysis): defined as achievement of final in-scaffold residual stenosis of <30% by visual estimation and TIMI Grade-3 flow with any device.

Procedural success (patient level analysis): defined as all lesions achieved lesion success after PCI procedure without the occurrence of major adverse cardiac events during the hospital stay (maximum of 7 days).

2.2 Clinical endpoints [1 month, 6 months, 1, 2, 3, 4 and 5 years]

Composite endpoints

Target lesion failure (TLF), including cardiac death, target vessel-myocardial infarction (MI), or clinical indicated target lesion revascularisation (CI-TLR).

Patient-oriented composite endpoint (PoCE), including all-cause death, all MI, or any revascularisation.

Other endpoints

Death. All deaths were considered cardiac unless an unequivocal non-cardiac cause could be established. Specifically, any unexpected death even in patients with coexisting potentially fatal non-cardiac disease (e.g. cancer, infection) was classified as cardiac.

Myocardial infarction.

1. **Periprocedural MI** (within 48 hours after PCI) was defined according to Absorb III trial definitions as below (1).

Baseline Biomarker	Biomarker Criteria
In patients with normal baseline CK-MB.	The peak CK-MB measured within 48 hours of the procedure rises to ⩾ 5 × ULN
In patients with elevated baseline CK-MB	1.) New ST elevation or ST depression ⩾0.5 mV or with new pathologic Q-waves in ⩾ 2 contiguous leads on ECG ⩾30 min and ⩽48h post-PCI; 2.) Post procedure TIMI 0/1 flow in a coronary artery or a side branch with reference vessel diameter ⩾2.0 mm which had TIMI 2-3 flow at baseline, or TIMI 2 flow in a major coronary artery or a side branch with reference vessel diameter ⩾3.0 mm which had TIMI 3 flow at baseline (core laboratory assessed); 3) Imaging evidence of a new loss of viable myocardium or a new regional wall motion abnormality.

2. **Spontaneous MI** was defined as elevation of troponin >ULN or CK-MB >ULN, plus one or more of the following must also be present: 1) symptoms

of ischemia; 2) ECG changes indicative of new ischemia (new ST-T changes or new LBBB); 3) development of pathological Q waves; 4) imaging evidence of a new loss of viable myocardium or a new regional wall motion abnormality.

Repeat revascularisation.

3. **Target lesion revascularisation (TLR)** was defined as any repeat percutaneous intervention of the target lesion or bypass surgery of the target vessel performed for restenosis or other complication of the target lesion. All TLR should be classified prospectively as clinical-indicated [CI] or not clinical-indicated by the investigator prior to repeat angiography. The target lesion was defined as the treated segment from 5 mm proximal to the scaffold and to 5 mm distal to the scaffold.
4. **Target vessel revascularisation (TVR)** was defined as any repeat percutaneous intervention or surgical bypass of any segment of the target vessel. The target vessel was defined as the entire major coronary vessel proximal and distal to the target lesion which includes upstream and downstream branches and the target lesion itself.
5. **Clinical indicated target lesion revascularisation (CI-TLR)** should be considered only if the diameter of the target lesion is $\geqslant$50% (as determined by the medical imaging core laboratory) and at least one of the following criteria is met during postoperative follow-up or during an unexpected coronary angiography visit: 1)A history of recurrent angina that may be related to target lesions; 2)Objective indications of ischemia (ECG changes) at rest or during exercise tests (or equivalent test) related to target lesions; 3)When the investigator determines that suspicious symptoms require relevant invasive diagnostic tests (e.g., Doppler flow reserve analysis or intra-coronary flow reserve analysis) and the diagnostic tests show abnormal results; 4)$\geqslant$70% diameter stenosis in the absence of any of these ischemia signs or symptoms (determined by core laboratory after coronary angiography).

Device thrombosis. Device (scaffold) thrombosis was defined according to Academic Research Consortium (ARC) criteria (2).

6. **Definite scaffold thrombosis** was considered to have occurred by either angiographic or pathologic confirmation. Angiographic confirmation of scaffold thrombosis was defined as the presence of a thrombus that originates in the scaffold or in the segment 5 mm proximal or distal to the scaffold, with at least 1 of the following criteria within a 48-hour time window: 1) acute onset of ischemic symptoms at rest; 2) new ischemic ECG changes that suggested acute ischemia; 3) typical rise and fall in cardiac biomarkers (refer to definition of spontaneous MI); 4) non-occlusive thrombosis (a spherical, ovoid, or irregular non-calcified filling defect surrounded by contrast material

on 3 sides or within a coronary stenosis seen in multiple projections, or persistence of contrast material within the lumen, or a visible embolization of intraluminal material downstream); 5) occlusive thrombus (TIMI 0 or TIMI 1 intra-scaffold or proximal to a scaffold up to the most adjacent proximal side branch or main branch (if it originates from the side branch). Pathological confirmation of scaffold thrombosis was defined as evidence of recent thrombus within the scaffold determined at autopsy or via examination of tissue retrieved following thrombectomy. **Note:** The incidental angiographic documentation of scaffold occlusion in the absence of clinical signs or symptoms was not considered a confirmed scaffold thrombosis (silent occlusion).

7. **Probable scaffold thrombosis** was considered to have occurred in the following cases: 1) any unexplained death within the first 30 days after intracoronary scaffold implantation (note: for patients presenting with STEMI, one might consider the exclusion of unexplained death within 30 days as evidence of probable scaffold thrombosis); 2) irrespective of the time after the index procedure, any MI that was related to documented acute ischemia in the territory of the implanted scaffold without angiographic confirmation of scaffold thrombosis and in the absence of any other obvious cause

Timing of scaffold thrombosis:

8. **Acute scaffold thrombosis:** 0-24 hours post scaffold implantation (note: time 0 was defined as the time point after the guiding catheter had been removed and the subject had left the catheterization lab)
9. **Subacute scaffold thrombosis:** >24 hours-30 days post scaffold implantation
10. **Early scaffold thrombosis:** 0-30 days post scaffold implantation including acute or subacute scaffold thrombosis
11. **Late scaffold thrombosis:** 31 days-1 year post scaffold implantation
12. **Very late scaffold thrombosis:** >1 year post scaffold implantation

2.3 Quantitative coronary angiography analysis methods

In each patient, the quantitative coronary angiography (QCA) of in-device segment (in-scaffold) and the peri-device segments (defined by a length of 5 mm proximal and distal to the scaffold edge—in-segment) were analysed by an independent imaging core laboratory in paired matched angiographic views after the procedure and at follow-up. The following QCA parameters were computed based on the methods previously described (3,4): minimal luminal diameter (MLD), reference vessel diameter, late lumen loss, and binary restenosis.

1. **Acute recoil.** For lesions without post-dilation: acute recoil was calculated by mean diameter (delivery balloon at the highest pressure) - mean luminal diameter (after implantation). For lesions with post-dilation: acute recoil was calculated by mean diameter (post- dilation balloon at the highest pressure) - mean luminal diameter (after post-dilation).
2. **MLD**, including in-scaffold, in-segment, proximal and distal MLD.
3. **DS (%)**, including in-scaffold, in-segment, proximal and distal DS.

4. **Angiographic binary restenosis**, defined as target lesion DS ⩾ 50% at follow up, including in-scaffold, in-segment, proximal and distal binary restenosis.
5. **Late lumen loss**, defined as the difference between MLD at post-procedure minus MLD at follow-up.
6. **Vasomotion**, defined as the change of mean lumen diameter prior to and post intracoronary injection of nitrate.

2.4 Intravascular ultrasound analysis methods

Intravascular ultrasound (IVUS) examination was required before, after device implantation and follow-up with a mechanical catheter (Boston Scientific, Natick, MA) at an automated pullback speed of 0.5 mm/s, the quantitative analysis was performed in 0.5-mm intervals in the scaffold segment and 5 mm proximal or distal segment according to the analysis method as previous report (3,5). The vessel area, scaffold area, lumen area, neointimal area were measured with QIvus 3.0 (Medis Medical Imaging, Leiden, the Netherlands). Volume obstruction was defined as neointima hyperplasia volume divided by scaffold volume. The scaffold absorption in IVUS was categorized into obvious and non-obvious according to the existence of widen strut shadowing of over 300 μm.

IVUS endpoints [post procedure; 6 months; 1, 2, and 3 years]:

1. **Vessel area** (minimal, mean), a discrete interface at the border between the media and the adventitia
2. **Lumen area** (minimal, mean), the area bounded by the luminal border
3. **Scaffold area** (minimal, mean), is measured by planimetry of the area bounded by the scaffold struts
4. **Neointimal area**, defined as scaffold area minus lumen area if all struts are apposed
5. **Volume obstruction**, defined as neointima hyperplasia volume divided by scaffold volume
6. **Late recoil**, calculated by scaffold area at post-procedure - scaffold area at follow-up

2.5 Optical coherence tomography analysis methods

Operation approach:

The optical coherence tomography (OCT) analysis was performed at imaging core laboratory based on the method previously described (3,6). The lumen and scaffold contours were obtained with a semiautomated detection algorithm by QIvus version 3.0 software packages (Medis, The Netherlands), and additional manual corrections were performed if necessary. At baseline, because the polymeric struts are translucent, the vessel wall lumen area can be imaged and delineated at the back (abluminal) side of the struts. At follow-up, the luminal area was drawn by semiautomatic detection, following the endoluminal contour of the neointima between and on top of the apposed struts. At three years, the appearance of the struts can be

detected as a black core which sometimes displays irregular high-intensity areas, possibly indicative of the presence of connective tissue that progressively replaces the proteoglycan that is initially present after the resorption of the polymer. In this case, the scaffold area was defined only by its black core, since the light-scattering frame is no longer distinguishable from surrounding tissue.

For malapposed struts, the endoluminal contour of the vessel wall behind the malapposed struts was used. At baseline, the scaffold area was measured by joining the middle point of the black core abluminal side of the apposed struts, or the abluminal edge of the frame borders of malapposed struts. The scaffold area was identical to the lumen area in the absence of malapposition and prolapse. At follow-up, the back (abluminal) side of the central black core was used to delimit the scaffold area, and each core was analysed per 0.4 mm. Scaffold late discontinuity was defined as new occurred isolated malapposed struts that cannot be integrated in the expected circularity of the device in at least one crosssection or those with an abrupt loss of longitudinal scaffold between two adjacent frames (7).

Moreover, three different situations deserve special consideration. First, incomplete strut apposition (ISA) was defined as a clear separation between the back (abluminal) side of the strut and the vessel wall. In case of malapposed struts, ISA area was delineated by the abluminal-side of the frame border of the malapposed strut (covered or uncovered) and the endoluminal contour of the vessel wall. Second, in a case of prolapse protruding between struts into the lumen at baseline, the prolapse area was estimated between the prolapsed contour (lumen contour) and the scaffold area. Third, an intraluminal defect free from the vessel wall (e.g. thrombus) also was quantified as an area. According to these findings, the blood flow area was defined as (scaffold area + ISA area) - (intraluminal strut areas + prolapse area + intraluminal defect).

Neointimal hyperplasia area was defined as (Scaffold area – [Lumen area + Black box area]) if all struts were apposed, while it was calculated as ([Scaffold area +ISA area + Malapposed strut with surrounding tissues] – [Lumen area + strut area]) in case of malapposed struts.

The thickness of the coverage was measured in every strut between the abluminal site of the strut core and the lumen. Because the strut thickness is 70 μm, the strut was considered as covered whenever the thickness of the coverage was above this threshold value. This method may slightly underestimate the thickness of the coverage since it does not take into account changes in the size of the strut core over time. Consequently, the percentage of uncovered struts may be slightly overestimated. Late absolute recoil was defined as scaffold area at post-procedure (X) – scaffold area at follow-up (Y). Late percent scaffold recoil was defined as $(X - Y)/X \times 100$. Percentage volume obstruction was defined as neointima hyperplasia volume divided by scaffold volume.

Eccentricity index was defined as the ratio of the minimum and maximum diameters in each frame; thereafter, the average of all eccentricity indexes was calculated. Symmetry index is calculated as (maximum scaffold diameter in a single frame - minimum scaffold diameter in a single frame) divided by the maximum

scaffold diameter. The maximum and minimum scaffold diameters in this calculation are possibly located in 2 different frames over the length of the device implanted

The OCT Healing Score is a weighted index that combines the following parameters (8):

1. Presence of intra-scaffold structure (ISS) is assigned a weight of "4."
2. Presence of both malapposed and uncovered struts (%MU) is assigned a weight of "3."
3. Presence of uncovered struts alone (%U) is assigned a weight of "2."
4. Presence of malapposition alone (%M) is assigned a weight of "1."

Neointimal Healing Score = (ISS × 4) + (%MU × 3) + (%U × 2) + (%M × 1).

OCT endpoints [post procedure; 6 months; 1, 2, and 3 years] (3,6):

1. **Neointimal thickness**, distance between the abluminal site of the strut and the lumen - strut thickness
2. **Proportion of covered struts**, percentage of covered struts based on struts level
3. **Incomplete strut apposition**, defined as 1 or more scaffold struts separated from the vessel wall. acquired late incomplete apposition is defined as incomplete apposition at follow-up that is not present after the procedure
4. **Percentage area obstruction**, calculated as neointima hyperplasia area/scaffold area × 100
5. **Healing score**, was calculated as a weighted index that including parameters as follow: presence of intra-scaffold structure (weight of 4), presence of both malapposed and uncovered struts (weight of 3), presence of uncovered struts alone (weight of 2), and presence of malapposition alone (weight of 1)
6. **Percentage of absorption**, was assessed using post-procedure radial heights of the sharply delineated struts as reference, struts at follow up were categorized into five groups according to height of expanded bow area generated during the degradation process(Supplementary Figure S4)
7. **Late recoil**, calculated by scaffold area at post-procedure - scaffold area at follow-up

Supplementary Appendix 3. Cases of TLR and TVR.

3.1 Four cases of TLR

Four cases of angiographic restenosis were observed after IBS suffered TLR, three of them were associated with mild recurrent symptoms, while the other one without functional significance. Review of these cases was instructive. In the first case a 3.5 × 15 mm IBS in the LAD developed neointimal hyperplasia throughout the entire IBS length. This was treated with a 3.5 × 30 mm Resolute (Medtronic) metallic DES, which also subsequently restenosed with a diffuse pattern, implying possible resistance to sirolimus analogues. In the second case a 3.0 × 15 mm IBS in the LAD developed diffuse restenosis at 6-month follow-up; the IBS was shown to have collapsed throughout its entire length with marked reduction in scaffold area, consistent with faster degradation of the IBS scaffold in humans than in rabbits. A metallic DES was implanted. In the third case a 3.0 × 23 mm IBS in LAD was shown at 12-month follow-up angiography to have developed a 1-mm long focal restenosis in the mid-scaffold. The stenotic segment was treated with a 3.0 × 25 mm drug coated balloon. The fourth case was adjudicated as restenosis by visual estimation at 3 year follow-up. The analysis found that the minimum lumen diameter (MLD) in scaffold was 1.69 mm and the reference lumen diameter was 3.2 mm, so the diameter stenosis by QCA was 47% which did not reach the restenosis standard (diameter stenosis$\geqslant$ 50%). In addition, after deducting proximal vessel stenosis, the quantitative flow ratio (QFR) at the target lesion was 0.83, which did not reach the ischemic diagnostic threshold ($\leqslant$0.80). Therefore, this case was considered as non-ischemia driven TLR.

3.2 One case of TVR (non-TLR)

One patient underwent TVR (non-TLR). The patient was implanted with a 3.0 × 18mm IBS scaffold in the middle of the LAD branch during the index procedure. Postoperative multi-position angiography showed good scaffold expansion, no dissection or hematoma was observed, and the TIMI flow grade was III. At 6 months post-procedure, the patient was followed up and angiographic results showed that the in-scaffold segment in LAD was patent but the dLAD was 100% occluded. dLAD was treated by balloon dilation, and the TIMI flow grade was III. Since the revascularisation was in the target vessel (LAD) but not the target lesion, it was classified as TVR.

Supplementary Table 1. Baseline characteristics and procedural results.

	All N=45	Cohort 1 N=28	Cohort 2 N=17
Age, years	53.2 ± 9.3	54.3 ± 8.7	51.4 ± 10.2
Male	35 (77.8%)	21 (75.0%)	14 (82.4%)
Current smoker	13 (28.9%)	6 (21.4%)	7 (41.2%)
Diabetes	12 (26.7%)	9 (32.1%)	3 (17.6%)
Hypertension	30 (66.7%)	20 (71.4%)	10 (58.8%)
Hyperlipidemia	43 (95.6%)	28 (100.0%)	15 (88.2%)
Previous myocardial infarction	6 (13.3%)	4 (14.3%)	2 (11.8%)
Previous stroke	4 (8.9%)	4 (14.3%)	0 (0%)
Previous PCI	5 (11.1%)	4 (14.3%)	1 (5.9%)
Unstable angina	22 (48.9%)	15 (53.6%)	7 (41.2%)
Left ventricular ejection fraction, %	63.5 ± 4.4	63.6 ± 3.3	63.5 ± 5.7
Target lesion location			
Left anterior descending	29 (64.4%)	17 (60.7%)	12 (70.6%)
Left circumflex	6 (13.3%)	4 (14.3%)	2 (11.8%)
Right coronary lesion	10 (22.2%)	7 (25.0%)	3 (17.6%)
AHA/ACC lesion class B2/C	18 (40.0%)	12 (42.9%)	6 (35.3%)
Pre-procedural QCA			
Reference vessel diameter, mm	2.98 ± 0.38	3.01 ± 0.40	2.94 ± 0.35
Minimum lumen diameter, mm	1.13 ± 0.38	1.16 ± 0.42	1.08 ± 0.31
Diameter stenosis, %	62.2 ± 11.3	61.6 ± 12.5	63.2 ± 9.4
Lesion length, mm	14.0 ± 4.2	13.6 ± 4.3	14.7 ± 4.0
Transradial approach	45 (100%)	28 (100%)	17 (100%)
Pre-dilation	45 (100%)	28 (100%)	17 (100%)
Maximum balloon diameter, mm	2.44 ± 0.30	2.44 ± 0.34	2.46 ± 0.20
Maximum balloon pressure, atm	13.1 ± 2.6	12.7 ± 2.6	13.8 ± 2.5
Scaffold diameter, mm	3.35 ± 0.34	3.37 ± 0.33	3.32 ± 0.35
Scaffold length, mm	20.0 ± 3.7	19.6 ± 3.8	20.5 ± 3.4
Post-dilation	42 (93.30%)	26 (92.9%)	16 (94.1%)
Maximum balloon diameter, mm	3.59 ± 0.32	3.60 ± 0.36	3.58 ± 0.25
Maximum balloon pressure, atm	17.1 ± 2.5	17.4 ± 2.8	16.5 ± 2.0

Procedural complications	0 (0%)	0 (0%)	0 (0%)
Postprocedural QCA			
Minimum lumen diameter, mm			
In-scaffold	2.78 ± 0.36	2.79 ± 0.34	2.77 ± 0.40
In-segment	2.55 ± 0.39	2.60 ± 0.38	2.47 ± 0.39
Diameter stenosis, %			
In-scaffold	9.3 ± 6.5	9.5 ± 6.8	9.1 ± 6.2
In-segment	14.3 ± 7.3	13.6 ± 7.0	15.5 ± 7.9
Acute gain, mm			
In-scaffold	1.65 ± 0.45	1.64 ± 0.51	1.68 ± 0.34
In-segment	1.42 ± 0.45	1.45 ± 0.52	1.39 ± 0.30
Acute recoil, mm	0.12 ± 0.08	0.11 ± 0.06	0.12 ± 0.11
Device success	45 (100%)	28 (100%)	17 (100%)
Lesion success	45 (100%)	28 (100%)	17 (100%)
Clinical success	45 (100%)	28 (100%)	17 (100%)

Data are mean ± SD or number (%). AHA/ACC=American Heart Association/American College of Cardiology. PCI=percutaneous coronary intervention. QCA=quantitative coronary angiography.

Supplementary Table 2. Medications at discharge and up to 3-year follow-up.

	Pre-procedure	Discharge	6 Months	1 Year	2 Years	3 Years
Dual antiplatelet therapy	97.8% (44/45)	100% (45/45)	97.8% (44/45)	93.3% (42/45)	64.4% (29/45)	62.2% (28/45)
Aspirin	100% (45/45)	100% (45/45)	100% (45/45)	100% (45/45)	100% (45/45)	97.8% (44/45)
P2Y12 inhibitor	100% (45/45)	100% (45/45)	97.8% (44/45)	91.1% (41/45)	64.4% (29/45)	64.4% (29/45)
Clopidogrel	95.5% (43/45)	91.1% (41/45)	86.7% (39/45)	80% (36/45)	51.1% (23/45)	51.1% (23/45)
Ticagrelor	11.1% (5/45)	17.8% (8/45)	20.0% (9/45)	20.0% (9/45)	17.8% (8/45)	17.8% (8/45)
ACE inhibitor or ARB	31.1% (14/45)	33.3% (15/45)	28.9% (13/45)	31.1% (14/45)	22.2% (10/45)	22.2% (10/45)
Beta-blocker	77.8% (35/45)	75.6% (34/45)	75.6% (34/45)	77.8% (35/45)	77.8% (35/45)	68.9% (31/45)
Calcium channel antagonist	42.2% (19/45)	42.2% (19/45)	48.9% (22/45)	46.7% (21/45)	46.7% (21/45)	46.7% (21/45)
Statin	97.8% (44/45)	97.8% (44/45)	100% (45/45)	100% (45/45)	100% (45/45)	95.6% (43/45)

Dual antiplatelet therapy (DAPT) includes aspirin plus clopidogrel or aspirin plus ticagrelor; ACE = angiotensin converting enzyme; ARB = angiotensin II–receptor blocker.

Supplementary Table 3. Paired quantitative coronary angiography results in cohort 1 and cohort 2.

	Cohort 1				Cohort 2			
	6 months (n=21)	**2 years (n=21)**	**Difference (95% CI)**	***p*-value**	**1 year (n=8)**	**3 years (n=8)**	**Difference (95% CI)**	***p*-value**
RVD, mm								
In-scaffold	2.99±0.35	3.04±0.36	-0.05 (-0.15,0.06)	0.35	2.99±0.24	3.00±0.35	-0.01 (-0.29,0.27)	0.93
In-segment	2.95±0.37	3.06±0.47	-0.11 (-0.27,0.05)	0.16	2.91±0.33	2.87±0.43	0.04 (-0.40,0.48)	0.82
MLD, mm								
In-scaffold	2.49±0.46	2.39±0.44	0.09 (0.00,0.19)	0.06	2.74±0.27	2.51±0.46	0.23 (-0.21,0.66)	0.26
In-segment	2.35±0.43	2.34±0.41	0.02 (-0.06,0.09)	0.65	2.47±0.28	2.36±0.41	0.11 (-0.20,0.41)	0.44
Diameter stenosis, %								
In-scaffold	16.9±13.1	21.2±10.8	-4.4 (-6.8,-2.0)	0.001	8.4±6.3	16.0±15.1	-7.6 (-20.7,5.5)	0.21
In-segment	20.0±11.4	23.1±10.9	-3.1 (-6.1,-0.1)	0.045	14.8±11.5	16.8±15.1	-2.0 (-14.3,10.3)	0.71
Binary restenosis								
In-scaffold	1 (4.5%)	1 (4.5%)	0.00 (-12.31,12.31)	1.00	0 (0.0%)	0 (0.0%)	-	-
In-segment	1 (4.5%)	1 (4.5%)	0.00 (-12.31,12.31)	1.00	0 (0.0%)	0 (0.0%)	-	-
Late lumen loss, mm								
In-scaffold	0.31±0.26	0.40±0.31	-0.09 (-0.19,0.00)	0.06	0.14±0.15	0.37±0.57	-0.23 (-0.66,0.21)	0.26
In-segment	0.25±0.29	0.27±0.35	-0.02 (-0.09,0.06)	0.65	0.10±0.10	0.21±0.38	-0.11 (-0.41,0.20)	0.44
Vasomotion, mm	0.13±0.13	0.13±0.10	0.00 (-0.07,0.07)	0.96	0.18±0.40	0.10±0.15	0.11 (-0.32,0.54)	0.52

Data are mean ± SD or number (%). CI=confidence interval; MLD=minimum lumen diameter; RVD=reference vessel diameter.

Supplementary Table 4. Paired intravascular ultrasound analysed results in cohort 1 and cohort 2.

	Cohort 1				Cohort 2			
	6 months (n=21)	**2 years (n=21)**	**Difference (95% CI)**	***p*-value**	**1 year (n=8)**	**3 years (n=8)**	**Difference (95% CI)**	***p*-value**
Mean vessel area, mm^2	17.7±3.5	17.4±3.6	0.30 (-0.44,1.04)	0.41	19.6±2.9	20.4±4.0	-0.75 (-2.33,0.84)	0.30
Minimum vessel area, mm^2	14.4±2.9	13.5±2.7	0.91 (0.12,1.69)	0.03	15.4±2.2	15.6±3.4	-0.28 (-1.58,1.01)	0.62
Mean lumen area, mm^2	8.09±1.74	7.61±2.08	0.47 (-0.04,0.98)	0.07	9.36±1.27	8.62±2.29	0.74 (-0.69,2.18)	0.26
Minimum lumen area, mm^2	5.88±1.51	5.09±1.28	0.79 (0.32,1.26)	0.002	7.07±0.70	5.73±1.35	1.34 (0.31,2.36)	0.02
Mean plaque area, mm^2	9.66±2.24	9.83±1.95	-0.17 (-0.78,0.44)	0.57	10.28±1.99	11.77±2.54	-1.49 (-2.37,-0.61)	0.005
Mean scaffold area, mm^2	9.01±1.72	9.00±2.09	0.01 (-0.68,0.69)	0.99	10.14±1.45	10.51±2.75	-0.37 (-2.07,1.32)	0.62
Minimum scaffold area, mm^2	7.17±1.32	6.39±1.38	0.79 (0.13,1.44)	0.02	7.81±0.88	7.82±2.20	-0.01 (-1.38,1.36)	0.99
Neointimal hyperplasia area, mm^2	0.73±0.43	1.17±0.87	-0.45 (-0.82,-0.08)	0.02	0.68±0.34	1.75±0.77	-1.07 (-1.53,-0.60)	0.001
Area obstruction, %	10.9±4.95	15.9±9.06	-5.00 (-8.67,-1.33)	0.01	8.09±1.92	18.3±5.21	-10.24 (-13.75,-6.74)	0.0002
In-scaffold volumetric obstruction, %	10.7±5.06	15.7±8.93	-4.97 (-8.64,-1.30)	0.01	8.08±1.89	17.8±5.22	-9.74 (-13.40,-6.08)	0.0004
Mean recoil area, mm^2	0.45±0.70	0.46±1.91	-0.01 (-0.69,0.68)	0.99	-0.51±1.02	-0.88±2.63	0.37 (-1.32,2.07)	0.62
Recoil area, %	4.46±6.84	3.31±20.74	1.16 (-6.73,9.04)	0.76	-6.24±12.21	-10.2±27.0	3.98 (-13.31,21.26)	0.60

Data are mean ± SD or number (%).

Supplementary Table 5. Paired optical coherence tomography analysed results in cohort 1 and cohort 2.

	Cohort 1				Cohort 2			
	6 months	**2 years**	**Difference (95% CI)**	***p*-value**	**1 year**	**3 years**	**Difference (95% CI)**	***p*-value**
Strut level	N=9172	N=8299			N=3288	N=3231		
Mean thickness of strut coverage, μm	182.9±124.6	183.0±107.1	1.3 (-1.7,4.3)	0.40	131.4±69.5	279.7±148.5	-141.3 (-146.6,-136.0)	<0.0001
Incomplete strut apposition, %	6 (0.1%)	0 (0.0%)	-	0.03	1 (0.0%)	0 (0.0%)	-	1.00
Late acquired incomplete strut apposition, %	0 (0%)	0 (0%)	-	1.00	0 (0%)	0 (0%)	-	1.00
Cross-section level	N=1079	N=1062			N=388	N=416		
Neointimal area, mm^2	1.58±0.83	1.58±0.74	0.05 (0.00,0.11)	0.07	1.23±0.53	2.75±1.22	-1.48 (-1.59,-1.37)	<0.0001
Proportion of covered struts, %	1076 (99.7%)	1062 (100.0%)	-	0.12	388 (100.0%)	416 (100.0%)	-	1.00
Lesion level	N=21	N=21			N=8	N=8		
Mean scaffold area, mm^2	9.13±1.92	9.15±2.28	-0.02 (-0.50,0.47)	0.94	10.48±1.61	10.74±2.86	-0.26 (-1.99,1.48)	0.74
Minimum scaffold area, mm^2	7.28±1.41	5.99±1.41	1.29 (0.90,1.69)	<0.0001	8.18±1.42	7.51±2.13	0.67 (-0.62,1.96)	0.26
Mean scaffold diameter, mm	3.39±0.36	3.37±0.42	0.01 (-0.08,0.11)	0.77	3.64±0.27	3.66±0.48	-0.02 (-0.30,0.27)	0.89
Minimum scaffold diameter, mm	3.16±0.35	3.10±0.38	0.06 (-0.03,0.15)	0.17	3.38±0.26	3.39±0.43	-0.01 (-0.26,0.24)	0.93
Mean luminal area, mm^2	7.58±2.04	7.62±2.40	-0.04 (-0.54,0.45)	0.86	9.28±1.32	8.03±2.32	1.25 (-0.19,2.68)	0.079
Minimum luminal area, mm^2	5.16±1.86	4.43±1.53	0.73 (0.30,1.16)	0.0020	6.90±1.18	4.55±1.59	2.35 (1.08,3.63)	0.0033
Area obstruction, %	18.1±7.6	18.1±7.9	0.07 (-2.86,3.00)	0.96	11.7±2.2	25.4±6.5	-13.6 (-19.1,-8.1)	0.0006
Healing score*	0.13±0.42	0.00±0.00	0.13 (-0.06,0.33)	0.17	0.03±0.08	0.0±0.0	-0.04 (-0.21,0.14)	0.65
Absolute late recoil, mm^2	-0.03±1.13	-0.09±1.73	0.06 (-0.45,0.56)	0.82	-0.95±1.07	-1.20±2.48	0.26 (-1.48,1.99)	0.74
Late recoil, %	-0.45±11.95	-1.27±19.20	0.81 (-5.35,6.97)	0.79	-11.19±14.30	-13.43±26.01	2.23 (-15.90,20.36)	0.78
Absorption, %	34.3±12.2	82.3±10.0	-48.5 (-54.0,-42.9)	<0.0001	49.18±11.29	95.38±3.83	-46.2 (-55.8,-36.6)	<0.0001

Data are mean ± SD or number (%). *Healing score = (presence of intra-scaffold structure × 4) + (presence of both malapposed and uncovered struts × 3) + (presence of uncovered struts alone × 2) + (presence of malapposition alone × 1).

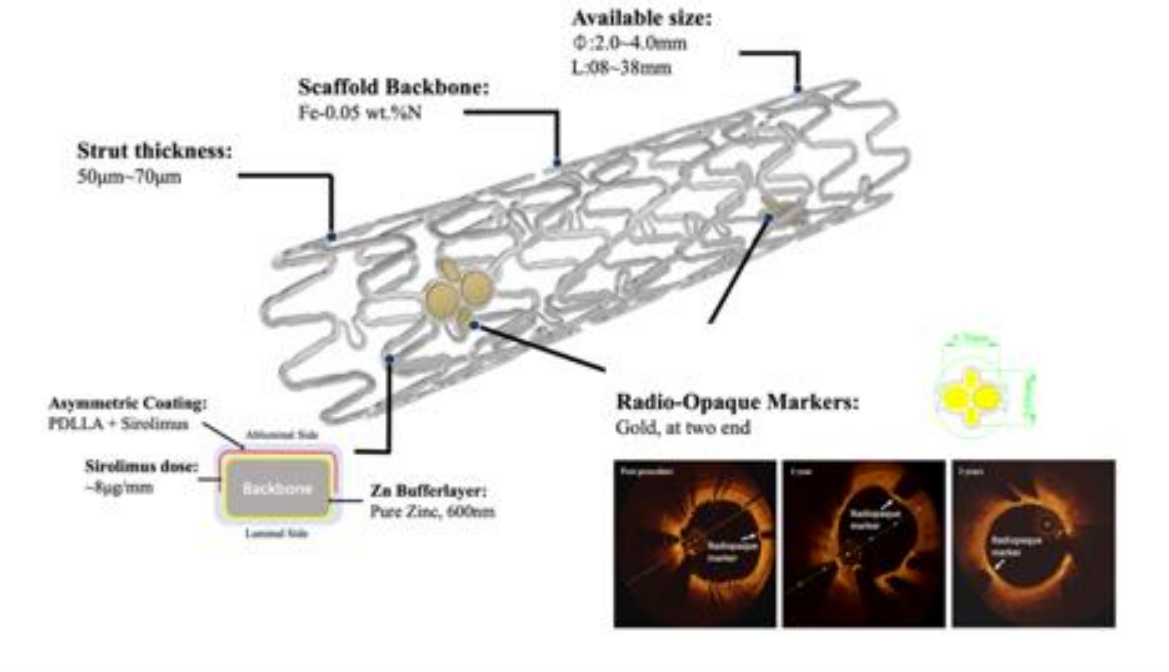

Supplementary Figure 1. Device description.
IBS = iron bioresorbable coronary scaffold; PDLLA = poly-D, L-lactic acid.

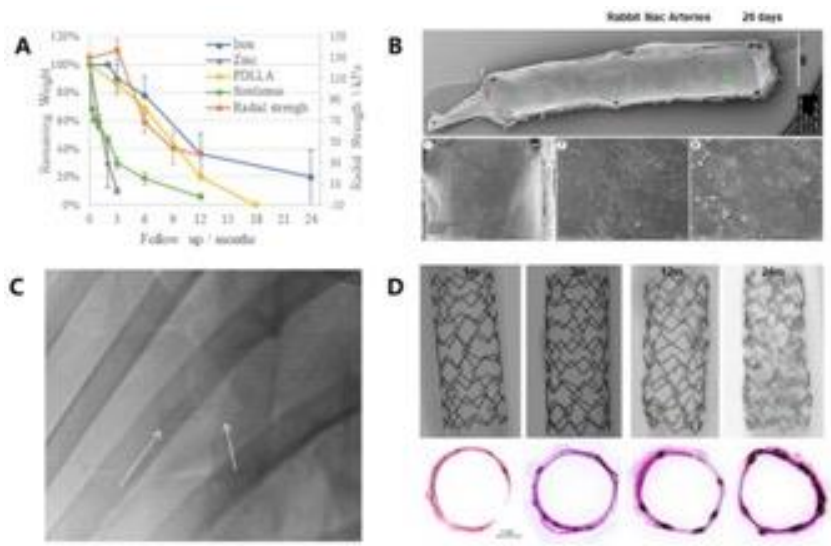

Supplementary Figure 2. Experimental animal results.
A) Corrosion profile and radial strength of the IBS scaffold after implantation in rabbit iliac arteries and abdominal aorta; B) SEM images of endothelial coverage of IBS scaffold after 28 days implantation in rabbit iliac artery; C) IBS scaffold outline under the X-ray after implantation in porcine coronary; D) Micro-CT images and hematoxylin and eosin (H&E) staining images of the IBS scaffold after implantation in rabbit iliac arteries and abdominal aorta at 1, 3, 12 and 24 months.

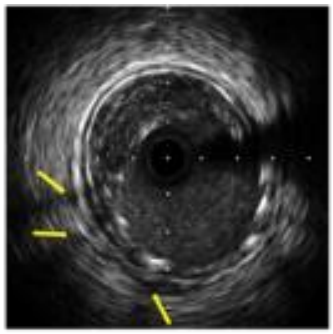

Struts without widened shadowing

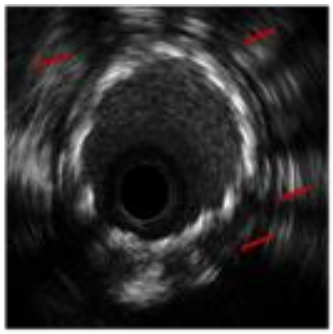

Struts with widened shadowing

	6 months Struts, N=4411	1 year Struts, N=2761	2 years Struts, N=2932	3 years Struts, N=1818
Struts with widened shadowing	7.4% (328)	35.7% (987)	59.8% (1754)	78.1% (1419)
Struts without widened shadowing	92.6% (4083)	64.3% (1774)	40.2% (1178)	21.9% (399)

Supplementary Figure 3. Scaffold absorption as assessed by IVUS.

Time	Post-Implantation and Before Iron Degradation	At follow-up				
Type	Type 0	Type 1*	Type 2*	Type 3*	Type j*	Type j+1†
Characteristics	Radial height of the original sharply delineated & highlight small strut area is around T_0; Degradation d0 is 0%	Radial height T_1 of the slightly deformed or dimmed small strut area is around T_0; Degradation d_1 is around 0%	Radial height T_2 of the small bow area delineated by the dim light degradation products is around $2T_0$; Degradation d_2 is around 20%	Radial height T_3 of the expanded bow area delineated by the dim light degradation products is around $3T_0$; Degradation d_3 is around 50%	Radial height T_j of the significantly expanded bow area delineated by the dim light degradation products is no less than $4T_0$; Degradation d_j is around 100%	Bioresorbed-Indiscernable Degradation d_j+1 is 100%
Typical Image		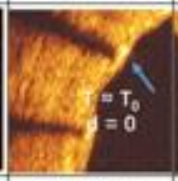				
6 months (N=12,122)	12,790(100.0%)	4,370(34.2%)	4,517(35.3%)	1,630(12.7%)	1,605(12.6%)	668(5.2%)
1 year (N=7,072)	8,127(100.0%)	1,383(17.0%)	2,350(28.9%)	1,454(17.9%)	1,885(23.2%)	1,055(13.0%)
2 years (N=8,299)	10,628(100.0%)	424(4.0%)	979(9.2%)	1,379(13.0%)	5,517(51.9%)	2,329(21.9%)
3 years (N=3,231)	4,241(100.0%)	6(0.1%)	59(1.4%)	333(7.9%)	2,833(66.8%)	1010(23.8%)

*Using the post-procedure strut number ($N_{post\text{-}procedure}$) as reference.
†$N_{Type\ j+1} = N_{post\text{-}procedure} - (N_{Type\ 1} + N_{Type\ 2} + N_{Type\ 3} + N_{Type\ j})$.
T: the radial height of the bow area formed after iron degradation; d: the iron degradation degree.
Note: To better estimate the true degradation rate, linear interpellation was performed between pairs of T_j—d_j, e.g. T_0 — 0%, $2T_0$ — 20%, $3T_0$ — 50% and $4T_0$ — 100%.
This table describes the frequency of each resorption category on OCT and percentage of struts for each resorption type. N is the number of struts observed at follow-up; N=Type 1+Type 2+Type 3+Type j. We defined the struts as Type j+1 if it is not visible on OCT; Type j+1=Type 0-N.

Supplementary Figure 4. Scaffold absorption as assessed by OCT.
Scaffold absorption by OCT was analysed using a semi-quantitative method.

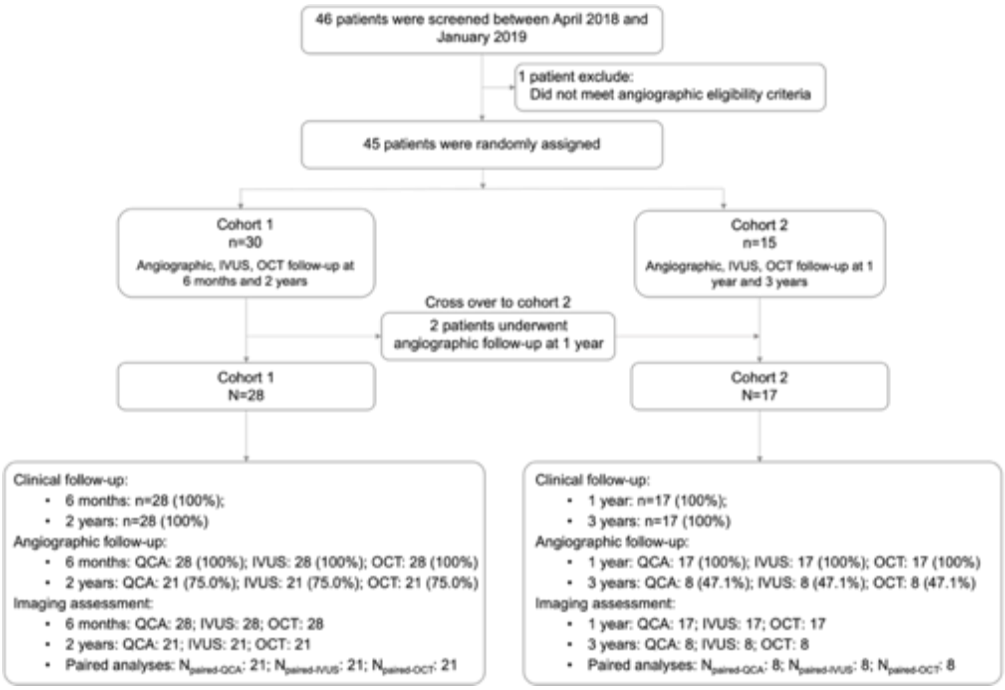

Supplementary Figure 5. Study flowchart.
QCA=quantitative coronary angiography; OCT=optical coherence tomography; IVUS=intravascular ultrasound

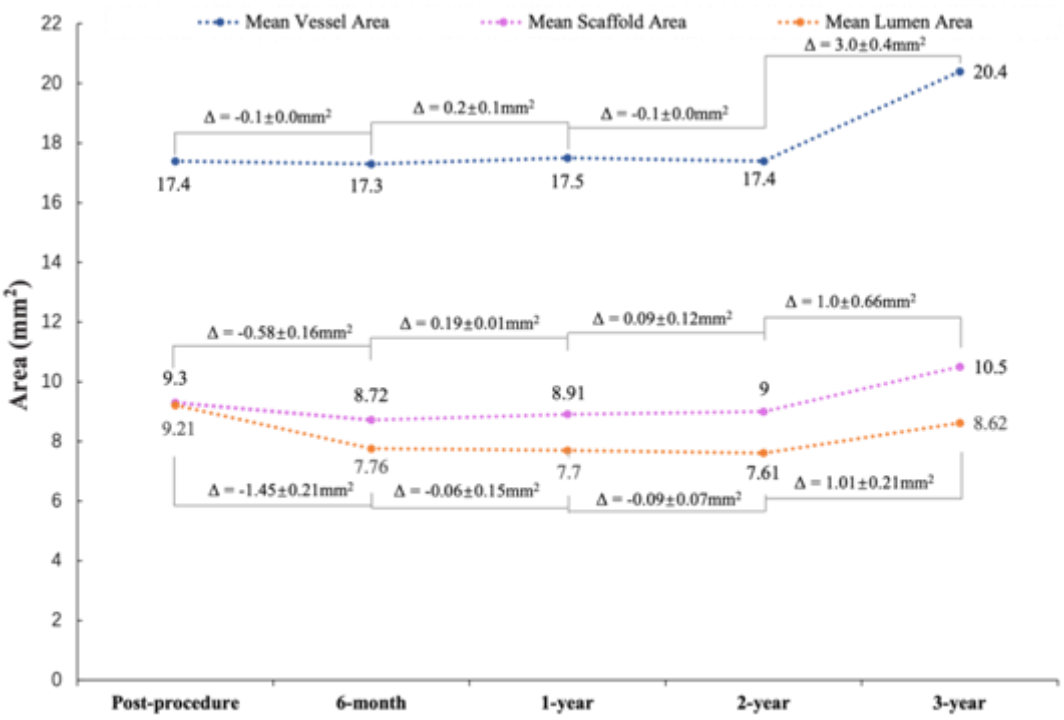

Supplementary Figure 6. Serial IVUS assessments up to 3-year follow-up.
The blue line illustrates mean vessel area changes; the purple line illustrates mean scaffold area changes; the orange line illustrates mean lumen area changes.

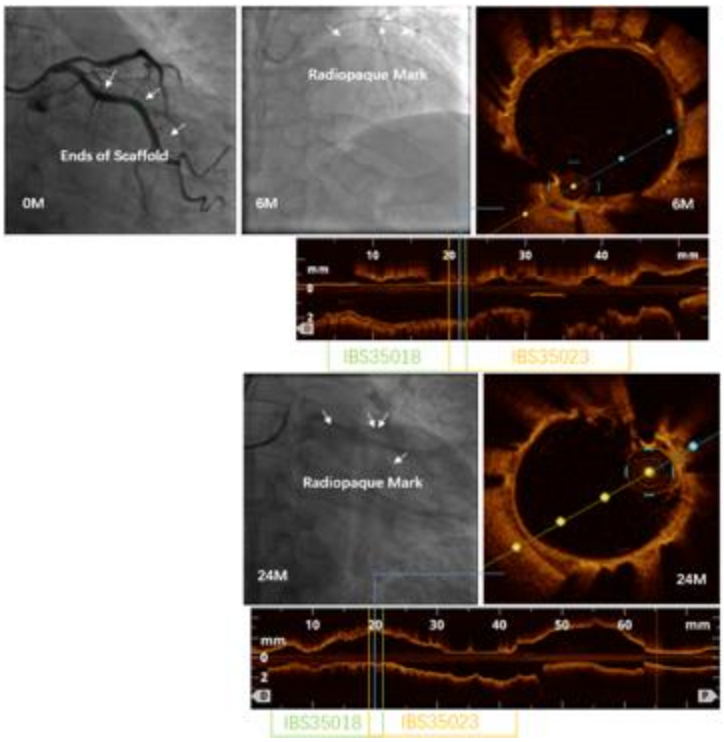

Supplementary Figure 7. Six-month and two-year imaging follow-up of a patient with the bailout IBS.

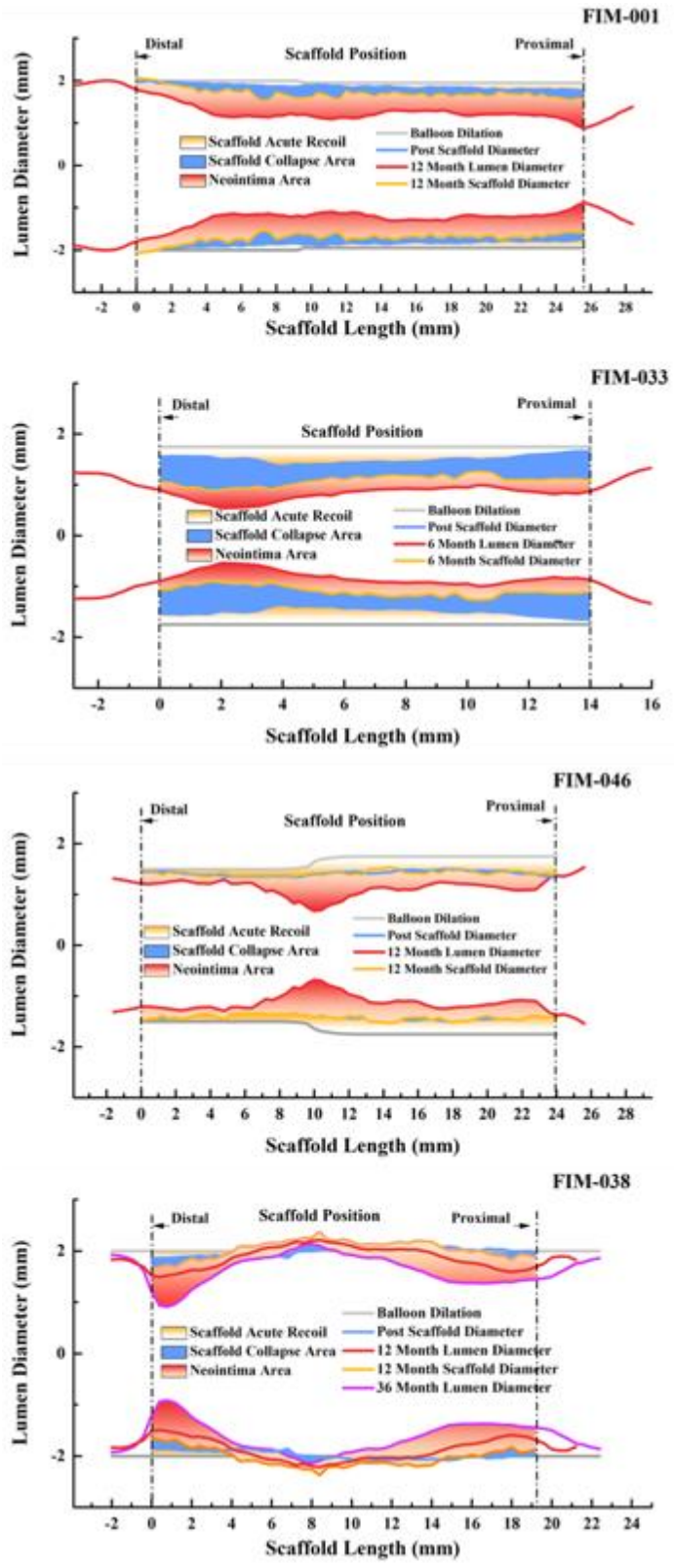

Supplementary Figure 8. OCT assessment in four cases undergoing target lesion revascularisation.

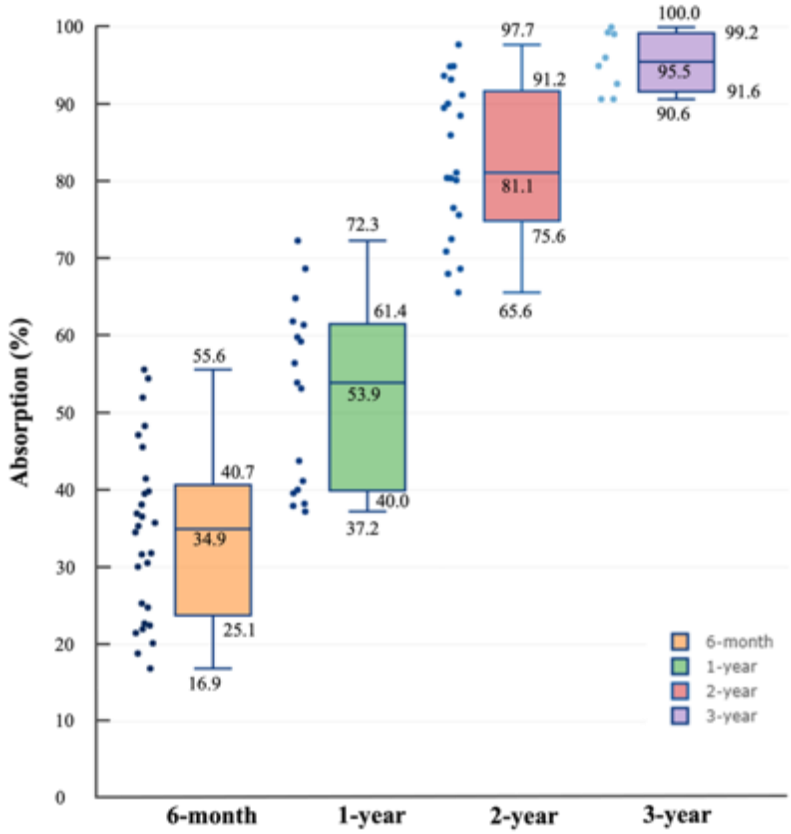

Supplementary Figure 9. Scaffold absorption assessed by OCT.

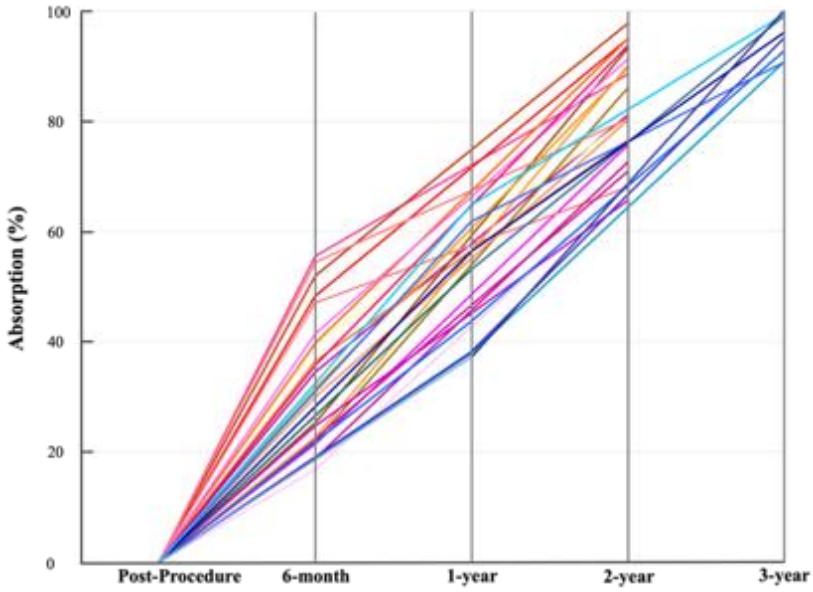

Supplementary Figure 10. Scaffold absorption assessed by OCT (paired measurements).